European Journal of Pharmaceutics and Biopharmaceutics 176 (2022) 54–74

Contents lists available at ScienceDirect

European Journal of Pharmaceutics and Biopharmaceutics

journal homepage: www.elsevier.com/locate/ejpb

Managing antibody stability: Effects of stressors on Ipilimumab from the commercial formulation to diluted solutions

Benedetta Fongaro [a], Valentina Cian [a], Francesca Gabaldo [a], Giorgia De Paoli [b], Giorgia Miolo [a,*], Patrizia Polverino de Laureto [a,*]

[a] Department of Pharmaceutical and Pharmacological Sciences, Via Marzolo, 5, 35131 Padova, Italy
[b] Molecular and Clinical Medicine, School of Medicine, University of Dundee Nethergate, Dundee, Scotland DD1 4HN, UK

ARTICLE INFO

Keywords:
Monoclonal antibody
Protein drug product
Mechanical stability
Artificial sunlight
Photostability
Dilution effect

ABSTRACT

The stability of the monoclonal antibody Ipilimumab, the active ingredient of Yervoy®, used for the treatment of different types of cancer, has been investigated. Shaking/temperature, light exposure and dilution, protein drug renowned stressors, were applied on a 30–45-day series of experiments to observe the physicochemical and biological behavior of the molecule. Ipilimumab demonstrated stability under shaking and heat up to 45 days, without any unfolding during the induced combined stressors. Under artificial sunlight, the mAb showed to be sensitive even under the minimum dose tested (720 kJ/m^2) with formation of aggregates, particularly when diluted in glucose solution. The light-induced soluble aggregates were higher in the case of diluted samples irradiated with much higher light doses (10460 kJ/m^2). The aggregation of Ipilimumab took place also by irradiating the non-diluted formulation, indicating that the excipients did not protect completely the drug from photodegradation. Amino acid oxidation and deamidation were found. Anyway, after irradiation with both light doses, soluble Ipilimumab maintained its typical β-sheets structure, and the tertiary structure was nearly maintained compared to the dark. As an additional stressor test, the effect of dilution on the formulation was monitored by using a saline solution (1 mg/mL Ipilimumab) applied during hospital infusion. After two days from dilution, the protein exhibited aggregation and chemical modifications including oxidation and deamidation. When stability conditions were compromised, the viability of human cell lines treated with the stressed formulation slight decreased suggesting low potential biological toxicity of the modified mAb. As this study has demonstrated the susceptibility of Ipilimumab to light, specific solutions, and excipients as well as the use of safe light in manufacturing, handling, and storage of this drug should be promoted. Moreover, the use of proper primary and secondary packaging should be indicated to avoid the detrimental effect of light on the mAb structure and efficacy. A detailed understanding of Ipilimumab physicochemical properties, integrity, and stability could assure the best storage and manipulation conditions for its safe and successful application in cancer therapy.

1. Introduction

Immunotherapy is one of the most recent cure of cancer, representing in some cases the first-line treatment [1,2]. Cancer growth, development and progression are associated with immune suppression and "immune checkpoints". Immune checkpoints or co-inhibitory molecules refer to inhibitory signals that immune cells must overcome to perform full effector functions [3]. The Cytotoxic T lymphocyte antigen-4 (CTLA-4) and programmed cell death protein 1 (PD-1) are key negative regulators of T cell activation and therefore two important immune checkpoints which have been identified to have a role in apoptosis, T cell activation, and maintenance of acquired immune system tolerance [3]. Monoclonal antibody (mAb) drugs, either immunoglobulins or immunoglobulin fragments, are designed to bind to antigens that are generally more numerous on the surface of cancer cells than healthy cells. [4,5]. They work in different ways, such as by directly attacking cancer cells or

Abbreviations: mAb, monoclonal antibody; SEC, Size exclusion chromatography; CD, Circular dichroism; ICH, International Conference on Harmonization; GDPs, glucose degradation products; HMW, high molecular weight.

* Corresponding authors.
E-mail addresses: giorgia.miolo@unipd.it (G. Miolo), patrizia.polverinodelaureto@unipd.it (P. Polverino de Laureto).

https://doi.org/10.1016/j.ejpb.2022.05.005
Received 2 March 2022; Received in revised form 5 May 2022; Accepted 7 May 2022
Available online 17 May 2022

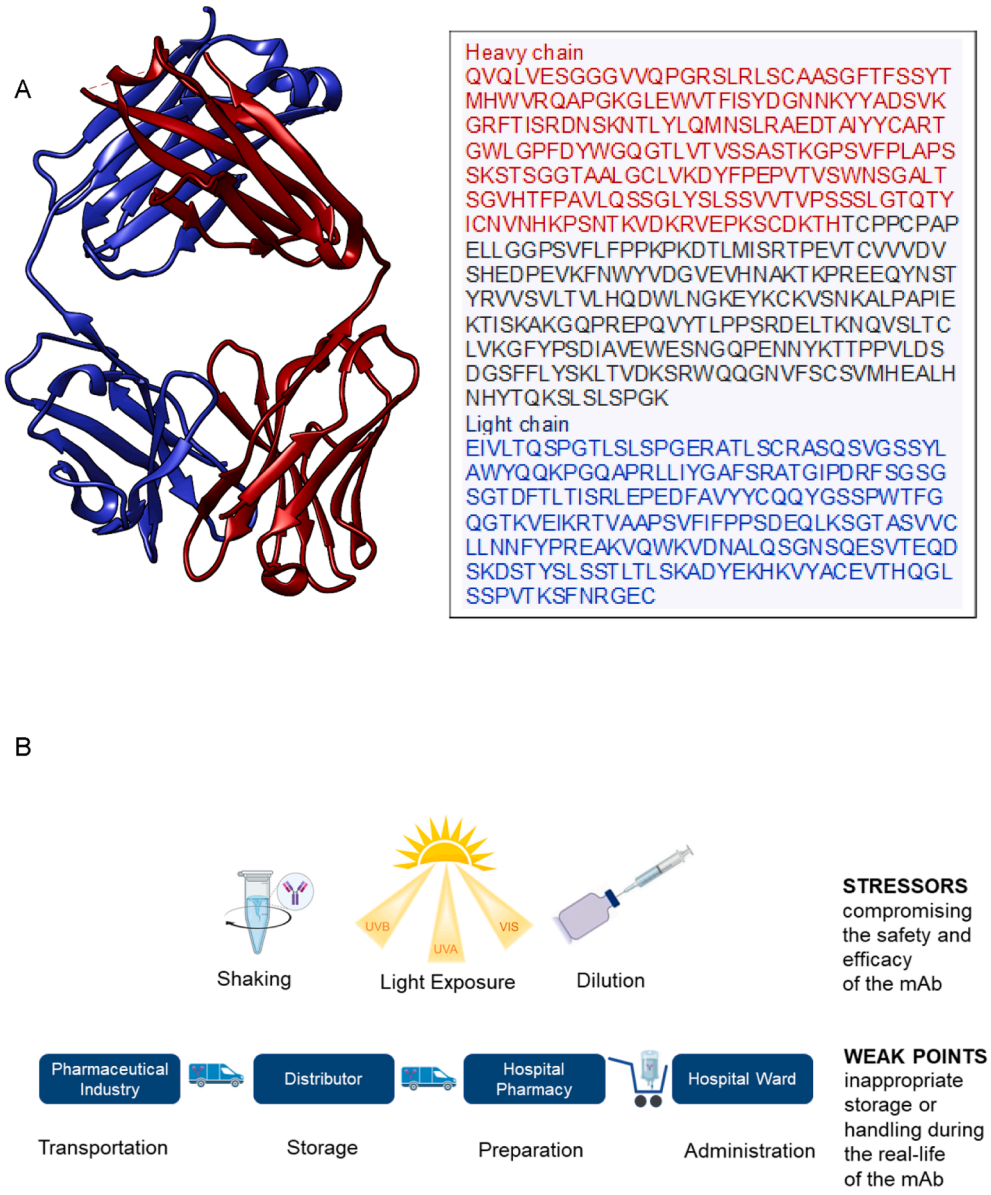

Fig. 1. Three-dimensional structure and amino acid sequence of Ipilimumab (PDB code 5-TRU 5-Xj3) (A). The structure was drawn by using the program Chimera. The heavy chain is reported in red, the light chain in blue. Stress factors and weak points during the handling of a protein drug (B). (For interpretation of the references to color in this figure legend, the reader is referred to the web version of this article.)

flagging cancer cells, triggering cell-membrane destruction, blocking cell growth, preventing blood vessel growth, and by blocking immune system inhibitors [6].

Ipilimumab, a CTLA-4-blocking mAb, has been approved by the US FDA in March 2011 for the treatment of several cancers, specifically melanoma, one of the most aggressive forms of human cancer [7–10]. By binding to CTLA-4, Ipilimumab reactivates pre-existing activated T cells and augments anti-tumor immunity in cancer [11]. Ipilimumab (5 mg/ml concentrate solution for infusion) is provided as Yervoy®by Bristol Myers Squibb. It is a fully-human mAb, composed of 1326 amino acids with a molecular weight of 145 kDa. It consists of four polypeptide chains; two identical heavy chains consisting of 448 amino acids and two identical light chains consisting of 215 amino acids, linked by inter-chain disulfide bonds (Fig. 1). The structure of the complex formed by the Ipilimumab Fab fragment and the N-terminal region of CTLA-4 was elucidated at a resolution of 3.0 Å [12] (Fig. 1). The Ab presents a glycosylation of the asparagine residue in position 298 that confers stability to the Ab structure [13]. The main carbohydrate chain is made up of galactose, mannose, N-acetylglucosammine, and fucose.

From a formulation point of view, Ipilimumab contains sodium chloride and pentetic acid to avoid metal-induced oxidation, the surfactant polysorbate 80 as stabilizer to prevent the impact of interfacial stress and mannitol to ensure proper osmolality of the drug formulation. It is advised to infuse Yervoy® (diluted or undiluted) immediately after opening [14] and, if not, to store the solution for up to 24 h in a refrigerator (2 °C to 8 °C) or at room temperature (20 °C to 25 °C) since the "*chemical and physical in-use stability of the undiluted or diluted concentrate (between 1 and 4 mg/ml) has been demonstrated for 24 h at 25 °C and 2 °C to 8 °C*".

Delivery, storage, and the choice of excipients in a formulation play a critical role in the development of a biological substance. To ensure the standards of quality, safety, and efficacy, the pillars of the pharmaceutical quality system, regulated by the International Conference on Harmonization (ICH) Q10 document (https://www.ema.europa.eu), define several stability tests that must be executed on drug materials and products. ICH Q5C is the document that regulates and defines the

parameters to evaluate the quality of biotechnological products. Since mAbs are prone to physical and chemical damages during manufacturing, storage, transport, reconstitution and/or administration, a careful analysis of the stability-influencing factors may help to avoid or mitigate these problems. Unfolding, aggregation and chemical modifications are the most common phenomena that can lead to a loss of protein conformation. Therefore, recognizing any factor affecting the quality and stability of mAb products is of utmost importance to prevent undesired degradation reactions over time, which can ultimately lead to a drop in their biological potency [15] (Fig. 1B).

Shaking could occur during transportation and shipping of the drug (either from the manufacturing place to the hospital or from compounding pharmacies to hospitals/healthcare institutes). This may lead to drug inactivation owing to an increase in the gas–liquid interface. Indeed, at the interface, the protein drug unfolds and maximizes exposure of hydrophobic residues to the air. Surface denaturation may also occur at the protein-container interface [16].

Another cause of biologics instability and degradation is light exposure, which can induce modifications of the primary, secondary, and tertiary structures of polypeptide chain. Under light, proteins can undergo oxidation, crosslinking, and fragmentation processes. Tryptophan, tyrosine, phenylalanine, cysteine and cystine, methionine, and histidine are the amino acids which are the most sensitive to photooxidation. The major pathways of photodegradation for proteins include direct UV light absorption followed by oxidation or photosensitization by internal or external chromophores present in the formulation [17]. Light absorption generates singlet or triplet excited states or radicals' formation. Amino acids can transfer their energy to molecular oxygen from the triplet state, generating very reactive oxygen species ($^1O_2$) [18]. Reactive free radicals can be formed also by protein hydrogen abstraction or electron transfer, generating peroxyl radicals, which can further react with the amino acid side chains. Tyrosine, histidine, and tryptophan peroxides propagate protein oxidation and trigger further oxidation via both radical and non-radical mechanisms. Furthermore, decomposition of hydroperoxides to radicals can ultimately result in backbone fragmentation [18]. In case of indirect photoreactions, a component of the formulation absorbs the UV or Vis radiations giving rise to one or more reactive species, which further react with the proteins. Tryptophan is particularly sensitive to this type of oxidation and can generate products such as kynurenine and N-formyl-kynurenine with photosensitizing properties higher than their parent molecule, and thus able to intensify the photooxidative damage of the entire protein structure [19]. Sreedhara et al have studied the effect of ambient light on two mAbs during processing and development observing site-specific Trp oxidation or aggregation and color change under mild light conditions. These processes occur at different extend depending on the tested mAb [20]. Oxidative processes can lead to reduced biological activity of the protein or formation of immunogenic species. Light exposure can occur at different stages of the biologics' journey, during manufacturing, during preparation at the hospital sites or while being administered [21]. The guidelines contained in ICH Q1B indicate how to carry out photostability tests on therapeutic proteins and to protect them from photooxidation by adding photosensitizers to the drug formulation such as polysorbate 80 [22].

Another critical point when handling mAb formulation is the dilution of the pharmaceutical form prior to administration. This operation results in dilution of the stabilizers, which leads the protein to be exposed to a new condition of instability. The indicated stability of diluted Ipilimumab would be only 24 h, recommended to avoid bacterial contamination, an issue that could lead to problems related to the handling in hospital wards [23]. Others have demonstrated that diluted formulation of mAbs can remain stable for several months [24]. However, attention must be paid to the medium used for the dilution. The commercially available 5% glucose for infusion solutions are sterilized by moist heat under pressure [25]. Heating glucose solutions cause the generation of various glucose degradation products (GDPs) [26], such as 5-hydroxymethylfurfural (5-HMF) [27]. The accumulation of 5-HMF caused by chronic administration may lead to acute toxicity in patients [28,29]. Moreover, 5-HMF might react with the drug product and induce damage of the active principle under light exposure [30].

The goal of this study is to provide information on the stability of Ipilimumab, formulated in the Yervoy® commercial product, in different stressed conditions. We have generated new information channels for improved drug stability, handling practices, and safety for patients under Yervoy® treatment. Following a systematic analytical approach trying to cover multiple aspects of the life of this protein drug, we investigated and recognized those critical steps where the stability of Ipilimumab could be compromised. mAb analyses were performed with a comprehensive approach to investigate how shaking, light exposure and dilution could affect Ipilimumab in Yervoy®. The tests were conducted on the non-diluted form of the initial pharmaceutical product and on the diluted therapeutically used concentration (i.e., 1 mg/mL), either in 0.9% saline solution or in 5% glucose solution to replicate the different types of infusion prepared and administered in the ward. A detailed understanding of Ipilimumab physicochemical properties, integrity, and stability could assure the best storage and manipulation conditions for its safe and successful application in cancer therapy.

2. Materials and methods

2.1. Materials

Commercially available Yervoy®, 5 mg/mL Ipilimumab, (Bristol-Myers Squibb) was purchased from a pharmacy. Catalase (CAT), trypsin and all other chemicals and reagents were of analytical grade and were obtained from Merck (Darmstadt, Germany).

2.2. Stressors

Shaking and temperature. The stability of Ipilimumab in the undiluted formulation was tested upon shaking, carried out at 750 rpm, at a temperature of 37 °C to amplify the molecular agitation stress in an Eppendorf Thermomixer Compact (Eppendorf, Hamburg, Germany). Sample aliquots were collected after 7 and 45 days of shaking and analyzed.

Exposure to artificial sunlight. The stability of Ipilimumab was tested after artificial solar light irradiation using a SunTest CPS + instrument (Atlas Material Testing Technologies GmbH, Linsengericht, Germany). The analyses were performed in accordance with the ICH Q1B guidelines (https://www.ich.org). The mAb was irradiated in non-diluted form; upon dilution in a sterile 5% glucose solution (1:5); in a lab-made 5% glucose solution (non-sterile; 1:5) and in a saline (0.9% sodium chloride) solution (1:5). Non-irradiated (dark) samples were used as a control. Two different doses of artificial solar light were applied: 720 kJ/m^2 (200 W hours/m^2) in the UV region (320–400 nm) as indicated in ICH Q1B guidelines; 10460 kJ/m^2 that was applied to maximize the light stressor, following the exposure criteria for "stress test" photostability studies, namely until significant degradation has occurred. The temperature was controlled by using a SunCool® device and kept at 22 °C.

Dilution. Yervoy® formulation was diluted in 0.9% sodium chloride solution according to the manufacturer's instructions or 5 % glucose (commercially available and lab-made) and its stability was tested up to 30 days. The assayed concentration was 1 mg/mL. To highlight the effects of the applied stressors, 0.1 mg/mL dilution was also tested in the dilution (as a stressor) experiments.

After stress treatments, aliquots of the samples were analyzed by means of Size exclusion chromatography (SEC), Dynamic light scattering (DLS), Native and SDS-PAGE, UV–Vis spectroscopy and second derivative calculations, far- and near-UV Circular Dichroism (CD), intrinsic fluorescence, and LC-MS/MS of the tryptic digest.

2.3. Size exclusion chromatography (SEC)

SEC was carried out in triplicates on an Ultra High-Performance Liquid Chromatography (UHPLC) (Agilent 1290 system, Santa Clara, CA, USA) with a TSK gel® UP-SW3000 column (4.6 × 300 mm, 2 μm; Tosoh Bioscience, Japan). The elution was conducted by 0.1 M sodium phosphate pH 6.8, containing 0.2 M Arg-HCl, and 0.05% sodium azide, at a flow rate of 0.35 mL/min. The detection was obtained at 280 nm. Sample aliquots (10 μL) were loaded at a concentration of 1 mg/mL, after centrifugation (15000 rpm per 15 min at 4 °C) to remove eventual insoluble particles. The calibration of the column was obtained by loading a mixture of proteins with known molecular weight (Thyroglobulin, γ-globulin, Ovalbumin, Ribonuclease A, p-aminobenzoic acid) (Fig. S1). Quantification was done by OriginPro 2018b software, integrating the area under the peaks after the baseline subtraction. The areas (Au) of the monomer and HMW species were calculated from SEC profiles and expressed as percentage of aggregated species ($Au_{HMW}/Au_{TOT} \times 100$).

2.4. Dynamic light scattering (DLS)

DLS measurements were performed on a Zetasizer Ultra (ZSU5700, Malvern instruments, Worcestershire, UK). Sample aliquots were loaded at a concentration of 1 mg/mL without further treatment. Each measurement is the result of the media between three runs. Scattering data were analyzed with the ZS Xplorer software and expressed as volume size distribution from which the values of hydrodynamic diameter were extracted.

2.5. Electrophoretic analyses

SDS-PAGE was performed on a 12 % T, 2.6% C, pH 8.8, acrylamide separating gel and a 5% acrylamide stacking gel according to Leammli (1970) [31]. Prior to loading onto the wells, samples were treated with an SDS-containing sample buffer and were boiled at 95 °C for 5 min. The electrophoretic run was performed at room temperature with a starting current intensity of 9 mA/slab followed by a 12 mA/slab. 5 μg of samples were loaded into each well. Native-PAGE was performed on a 10% acrylamide running and stacking gels. The electrophoretic run was performed at room temperature with a starting current intensity of 5 mA/slab, and then 20 mA/slab. The running buffer containing β-alanine 0.35 M and AcH 0.14 M, pH 4.3 was used to perform the electrophoretic analysis. All gels were hand-casted and the electrophoretic runs were performed in a Mini-PROTEAN® Tetra System (BIO-RAD Laboratories Inc., Hercules, California, USA) stained with a Coomassie Blue R-250 solution and destained with an H_2O, methanol, and acetic acid solution in a ratio of 50/40/10 (v/v/v).

2.6. Spectroscopic measurements

UV–Vis analyses were performed by a Lambda-25 spectrophotometer (Perkin Elmer, Shelton, CT, United States) in a 230–350 nm range, using a quartz cuvette with a 1 cm pathlength and a sample concentration of 0.1 mg/mL. The spectra were taken at scan speed of 200 nm/min, data pitch of 0.1 nm. The second derivative [32] was calculated by the software provided by the manufacturer. Circular dichroism (CD) measurements were performed on the samples diluted in the same conditions used for the stress tests to monitor mAb secondary and tertiary structure, by acquiring spectra in the far-UV (250–195 nm) and the near-UV (350–250 nm) range by a Jasco J-810 spectropolarimeter (Tokyo, Japan). Far-UV CD spectra were obtained at a sample concentration of 0.1 mg/mL using quartz cells with a 1 mm pathlength, whereas near-UV measurements were carried out at a 0.5 mg/mL protein concentration using quartz cells with a 5 mm pathlength. CD signal was expressed as the mean residue ellipticity $[\theta] = \theta_{obs} \cdot MRW/(10 \cdot l \cdot c)$, where θ_{obs} is the observed signal in degrees, MRW is the protein mean residue weight, l is the cuvette pathlength in cm, and c is the protein concentration in g/mL. The sample concentration was determined spectroscopically on the soluble protein in the supernatant after centrifugation, by using a molar extinction coefficient 1.39 $mlmg^{-1}cm^{-1}$, calculated according to Gill and Von Hippel [33]. A Jasco ETC-273 fluorimeter (Tokyo, Japan) was used for intrinsic fluorescence measurements. Analyses were performed using a 1 cm pathlength quartz cuvette, at a 0.1 mg/mL concentration, testing the samples at 295 and 280 nm excitation wavelengths.

2.7. Fingerprinting analysis

Ipilimumab was subjected to an enzymatic fingerprinting. Samples were incubated for 1.30 h at 40 °C with a 50 mM Tris-HCl reducing buffer containing 6 M Guanidinium, pH 8.5; Tris(2-carboxyethyl) phosphine (TCEP) was added at a 1:10 ratio on Cys residues to allow the reduction of S-S bridges. Iodoacetamide was used to alkylate (carbamidomethylation) the free cysteine at a 1:10 ratio on Cys residues for 30 min in dark conditions at 22 °C. The buffer was changed with 100 mM ammonium bicarbonate by Amicon® Ultra 0.5 mL centrifugal filters (Merk Millipore Ltd., Ireland). Tryptic digestion was obtained at a 1:20 trypsin to mAb ratio (weight/weight). The reaction was left at 37 °C overnight and then stopped by freezing at −20 °C. Proteolytic mixtures were analyzed by LC-MS/MS, using a Xevo® G2-XS ESI-Q-TOF mass spectrometer (Waters Corporation, Milford, Massachusetts, USA). The UPLC analyses were carried out on an Acquity H-Class instrument (Waters Corporation, Milford, Massachusetts, USA) using an Agilent AdvanceBio Peptide Map (2.1x150mm × 2.7 μm; Santa Clara, CA, USA). The elution was performed at a flow of 0.2 mL/min eluted with the following acetonitrile/0.1% formic acid - water/0.1% formic acid gradient: 2–65%, 36 min, 65–98%, 2 min. Mass analyses were carried out at 1.5–1.8 kV capillary voltage and 30–40 V cone voltage.

2.8. Cell viability assay

Two different primary cultures of human cerebral microvascular endothelial cells, HBEC-5i (ATCC® No. CRL-3245™) and malignant melanoma cell, SK-MEL-28 (ATCC® No. HTB-72™) were incubated at 37 °C under 5% CO_2 for 2 days in 75 cm^2 flasks (NUNC, Roskilde, Denmark). For HBEC-5i the flasks were pre-treated with gelatin and a DMEM-F12 medium supplemented with 10% fetal bovine serum, 1% PS, 1% Gln and 0.8% human epidermal growth factor were used. For SK-MEL-28 DMEM-F12 medium was used supplemented with 10 % fetal bovine serum, 1% HEPES, 1% PS and 1% Gln. Confluent cells were detached using a trypsin-EDTA solution and then the cells were centrifuged at 100 × g for 5 min. After removing the supernatant, the cell pellets were re-suspended in fresh medium, counted in a Bürker Counting Chambers, and seeded at 5000 cells per well in 96-well plates (NUNC, Roskilde, Denmark) for the cell viability assay. Viability assay with Presto Blue (PB) reagent was performed according to the manufacturer's protocol. The cells in suspension were seeded at a concentration of 5000 cells/100 μL in a 96-well micro-titer plate. The irradiated lyophilized samples were suspended directly in the cell medium. After treating the cells for 24 h with different concentrations of mAb (0.67 mM, 3.36 mM), the changes in cell viability were detected using absorbance spectroscopy after 24 and 72 h of incubation. The absorbance was recorded at 570 nm after 3 h of cerebral endothelial and melanoma cells with PB reagent. To ensure that PB was not toxic to the cells and that it did not affect the measurements (especially after longer incubation times), the cells were also incubated without the antibody (following their 24 h attachment) and treated with PB.

2.9. Statistical analysis

All data were reported as means values ± standard deviation (SD) of triplicates. Statistical analysis using one-way ANOVA, with p-value < 0.05 as regarded statistically significant. The differences between

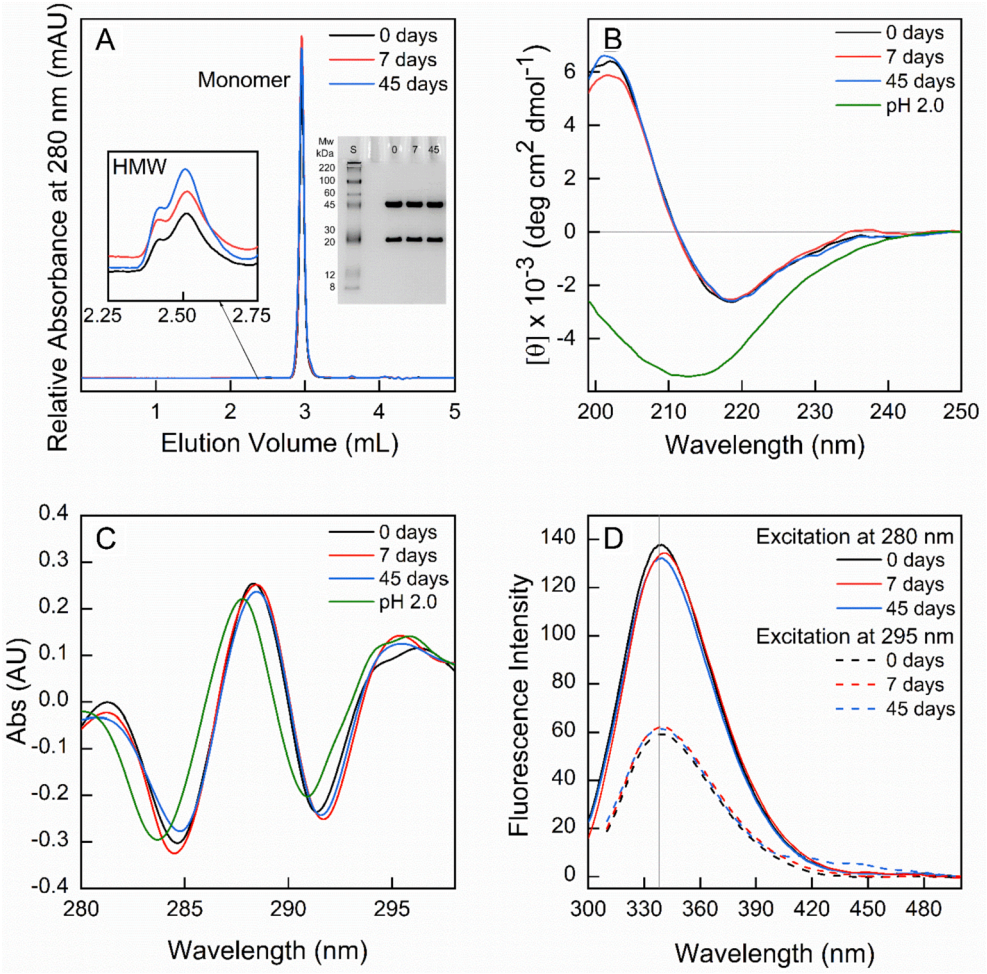

Fig. 2. Characterization of the effects of shaking and temperature on Ipilimumab in the original formulation monitored by SEC (A), far-UV CD (B), UV second derivative (C) and intrinsic emission fluorescence (D). The measurements were conducted after shaking the protein samples at 750 rpm up to 45 days at 37 °C. The results relative to 0 (black), 7 (red) and 45 (light blue) days are shown. In plot A, the left inset highlights the protein aggregates detected by SEC. The inset on the right shows the SDS-PAGE: lane 1, MW standard proteins (S); lane 2–4 mAb after 0, 7, and 45 days of incubation. The green line in panels B and C refers to the spectra of Ipilimumab obtained at pH 2.0. (For interpretation of the references to color in this figure legend, the reader is referred to the web version of this article.)

control and experimental samples were determined by *t*-test.

3. Results

3.1. Mechanical and temperature stress

Mechanical stress and temperature fluctuation are common during drug transportation. To detect the stability of Ipilimumab under a combination of these stressors, transportation was simulated with a vigorous shaking (750 rpm) with the combination of the temperature stress (37 °C). These emphasized conditions were applied to the mAb to better detect any alteration of the protein as a consequence of the stress. Aliquots of stressed and control samples were collected the day of the experiment (0), at day 7 and day 45 and analyzed by biophysical techniques. In SEC analysis, stressed Ipilimumab samples presented the same elution volume (2.96 mL) for the three days of collection (Fig. 2A). According to the calibration curve (Fig. S1), the above elution volume corresponded to a MW of ~ 81 kDa. This indicated an underestimation of the molecular mass, likely due to the intrinsic hydrophobicity of Ipilimumab which caused a slight modification of its elution time [34]. The zoomed (amplified 280-fold) window highlights the presence of high molecular weight species (HMW) just before the stress was applied. Since these species were also present in the commercial non-stressed solution, they clearly did not form under the thermomixer action. The areas of all peaks (Au_{TOT}) and HMW species (Au_{HMW}) were measured from SEC profiles and expressed as percentage of soluble aggregated species ($Au_{HMW}/Au_{TOT} \times 100$). At time 0 and after 7 days, this ratio was 0.31 and 0.33%, respectively, whereas after 45 days of incubation, it slightly increased to 0.40%. As regards the insoluble aggregates eventually removed by the centrifugation step before sample injection, they accounted for no more than 4% as calculated evaluating the protein peak areas (Au_{TOT}) in the SEC profile with respect the initial amount of the sample. In accordance with the SEC analyses, stressed samples did not exhibit the presence of aggregated species in SDS-PAGE (Fig. 2, inset), and only the two bands of the mAb, the first at ~ 50 kDa corresponding to the heavy chain, the second one at ~ 25 kDa for the light chain, were detected according to the expected molecular weight.

Spectroscopic measurements were performed to verify the effect of the stressor on the secondary and tertiary structure of Ipilimumab. Far-UV CD spectra (Fig. 2B) were recorded by using three different conditions. Black line represents non-stressed Ipilimumab, the red line indicates Ipilimumab after 7 days and the blue line corresponds to Ipilimumab after 45 days of combined shaking/temperature. It is clearly visible that the shape of the spectra, indicative of the presence of β-sheets structure, did not change after the mechanical stress. The far-UV CD spectrum of denatured Ipilimumab at pH 2.0 (green) is reported as a positive control. To gather information on the changes occurring in the micro-environment around Tyr and Trp residues [32] and the effect of the mechanical stress on the tertiary structure of Ipilimumab, the second derivative of the UV absorbance spectra were calculated, and also fluorescence measurements were performed on the same samples. The profiles obtained by the second derivative after 7 and 45 days of shaking of Ipilimumab at 37 °C appear overlapped (Fig. 2C), suggesting no extensive modification in the chemical environment and exposure of the aromatic amino acids during the mechanical stress. In Fig. 2D, the fluorescence spectra are shown. The maximal emission

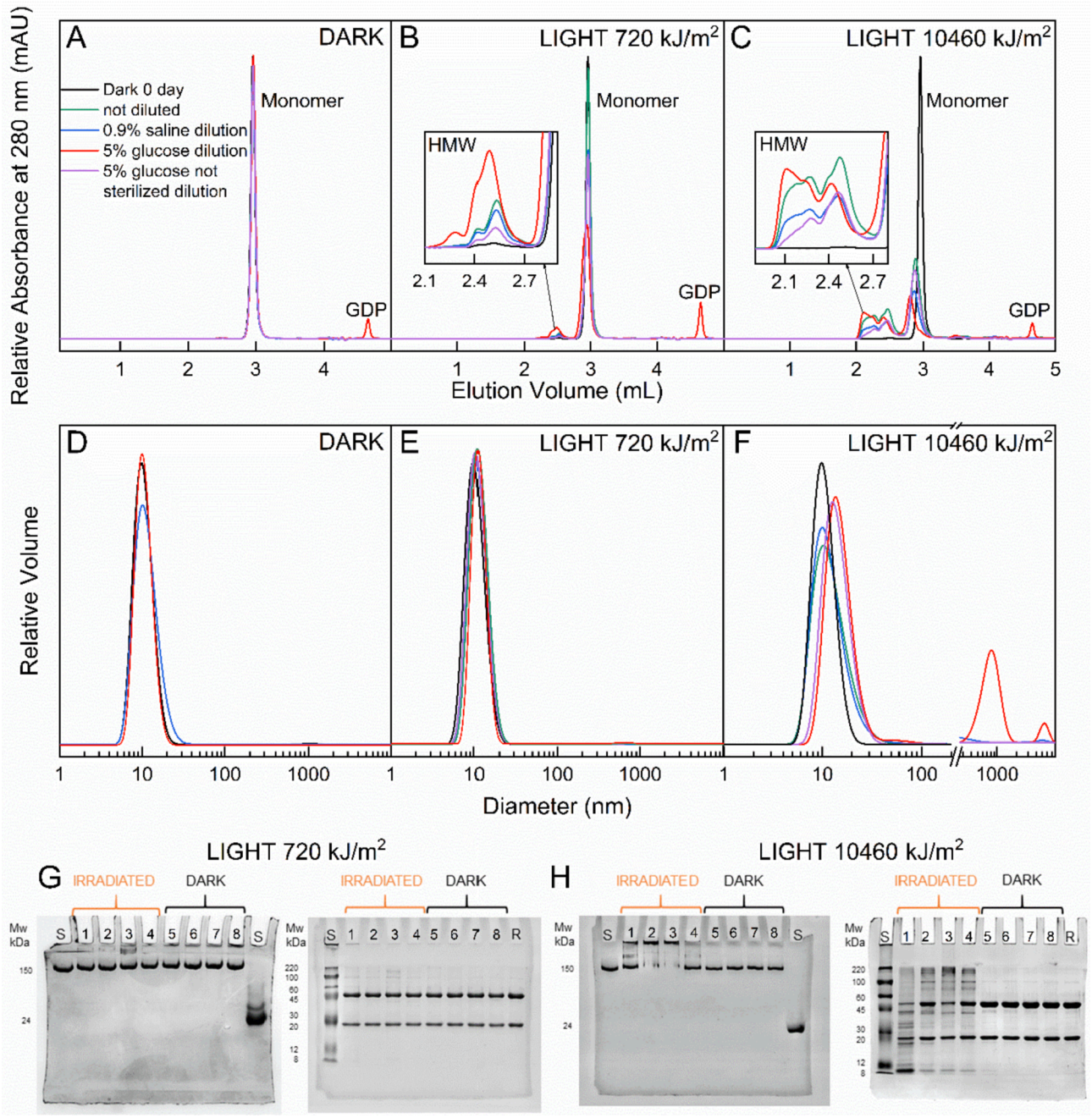

Fig. 3. Characterization of the effects of light exposure on the stability of Ipilimumab monitored by SEC (A-C), DLS (D-F), native- and SDS-PAGE (G, H, left and right, respectively). The measurements were conducted after exposure of the protein samples under 720 and 10460 kJ/m^2 of artificial sunlight. The diluted samples were analyzed after 0.9% saline dilution (light blue), 5% glucose dilution (red) and 5% not sterile glucose dilution (purple) in comparison to the not diluted one (green) and the dark control (black). As dark control, the mAb was diluted in the three different conditions and kept protected from light. The not diluted sample refers to the initial formulation (5 mg/mL), after irradiation and dilution with the mobile phase (1 mg/mL) just before the injection. Inserts in B and C report the zoom of the chromatogram from 2.0 to 3.0 mL of elution volume to highlight the formed aggregates. In F, the region centered at diameter higher than 500 nm was zoomed (25 x). HMW indicates the high molecular weight species. GDPs refers to glucose degradation products. Native- (left) and SDS- (right) PAGE of samples irradiated with 720 kJ/m^2 (G) and with 10460 kJ/m^2 (H) of artificial sunlight. (For interpretation of the references to color in this figure legend, the reader is referred to the web version of this article.)

wavelength at ~ 339 nm, correlated to Trp buried inside the molecular structure or folded protein, was observed in all conditions. The intensity of emission spectra decreased by exciting the protein at 295 nm where only Trp was selectively excited [35]. Overall, there was no change in the tertiary structure of the mAb as the environment of aromatic amino acids was kept unchanged. Based on these results, Yervoy® demonstrated stability under shaking and heat up to 45 days, with no alterations or unfolding during the induced stress.

3.2. Photostability

The intrinsic stability of Ipilimumab to light exposure was tested in the original formulation and diluted solutions as handled in the hospital pharmacy, by using two light doses. The irradiation under 720 kJ/m^2 corresponds to about 1–2 days of solar light exposure. The provided amount of artificial solar radiation of 10460 kJ/m^2, corresponding to about 21 days of solar light exposure, was applied to maximize the light

Table 1
Physical parameters deduced by SEC and DLS analyses (Fig. 3). Elution volumes and diameters of non-diluted and diluted Ipilimumab before (dark) and after irradiation with 720 and 10460 kJ/m^2 of artificial sunlight.

Samples	Irradiation (kJ/m^2)	Elution Volume (mL)	Diameter (nm)
dark	0	2.96	9.65 ± 0.17
not diluted	720	2.96	11.23 ± 0.55
0.9 % saline	720	2.96	11.23 ± 0.18
5 % glucose	720	2.94	11.23 ± 0.49
5 % not sterilized glucose	720	2.96	11.12 ± 0.15
not diluted	10,460	2.88	12.83 ± 0.51
0.9 % saline	10,460	2.86	12.82 ± 0.28
5 % glucose	10,460	2.80	13.06 ± 0.78
5 % not sterilized glucose	10,460	2.87	13.06 ± 0.58

stressor, following the exposure criteria for "stress test" photostability studies. The Yervoy® solution was irradiated upon dilution in sterile 0.9% NaCl solution (1:5), in sterile 5% glucose solution (1:5) and in a lab-made 5% glucose solution (non-sterile, 1:5). It is worth mentioning that this last condition is not recommended by the manufacturer's instructions, but it was investigated only for analytical purposes to evaluate the effect on glucose sterilization products related to the stability/photostability of the mAb [36].

Non-irradiated (protected from light) samples collected directly from their original vial (black and green lines) and diluted in the different buffers (blue, red and purple lines) exhibited the same elution volume when eluted in SEC (Fig. 3A, dark). In Fig. 3B, it is evident by SEC criteria that the mAb showed to be sensitive to simulated solar light even under the minimum dose tested (720 kJ/m^2). In the irradiated samples, the main peak, representing the monomer, exhibited a minor intensity with a concomitant increase of the high molecular species (HMW). For the 5% glucose solution (red line), a further increase of HMW species was observed. Moreover, there was a slight shift of the corresponding monomer elution volume towards higher MW values. Evaluating the area of the peaks, the amount of the formed soluble aggregates was 7.5% for the mAb diluted in 5% glucose (red line). In the case of not diluted, 0.9% saline diluted and 5% home-made diluted samples, this value ranged between 1.5 and 3%. In the red chromatogram, another peak eluting at 4.64 mL was visible already in the dark control. This peak could be attributed to a glucose degradation product (GDP), most likely generated during the heat sterilization of the glucose solution [26]. Therefore, SEC analysis was performed on the sample diluted in 5% glucose solution prepared in the lab without the sterilization step as in the industrial process. Under this condition, no peak was observed at 4.64 mL and the presence of aggregates was almost undetectable (Fig. 3B, purple line). In Fig. 3C, the results of the SEC analysis for the samples irradiated with 10460 kJ/m^2 are reported. An evident decrease of the intensity of the monomer peak with a concomitant increase of the HMW species was observed. The amount of soluble aggregates was higher for the glucose diluted mAb (red line; 34%) than other samples. In the case of the samples diluted in saline solution and in home-made glucose this value was between 12 and 20%. The insoluble aggregates in diluted mAb were between 31 and 32% of the initial irradiated sample, independently from the diluent used. Of interest, not diluted Ipilimumab formed only 3% of insoluble aggregates, whereas the amount of soluble aggregates was 29.5%, suggesting that different kind of HMW species were formed under irradiation. As the amount of HMW

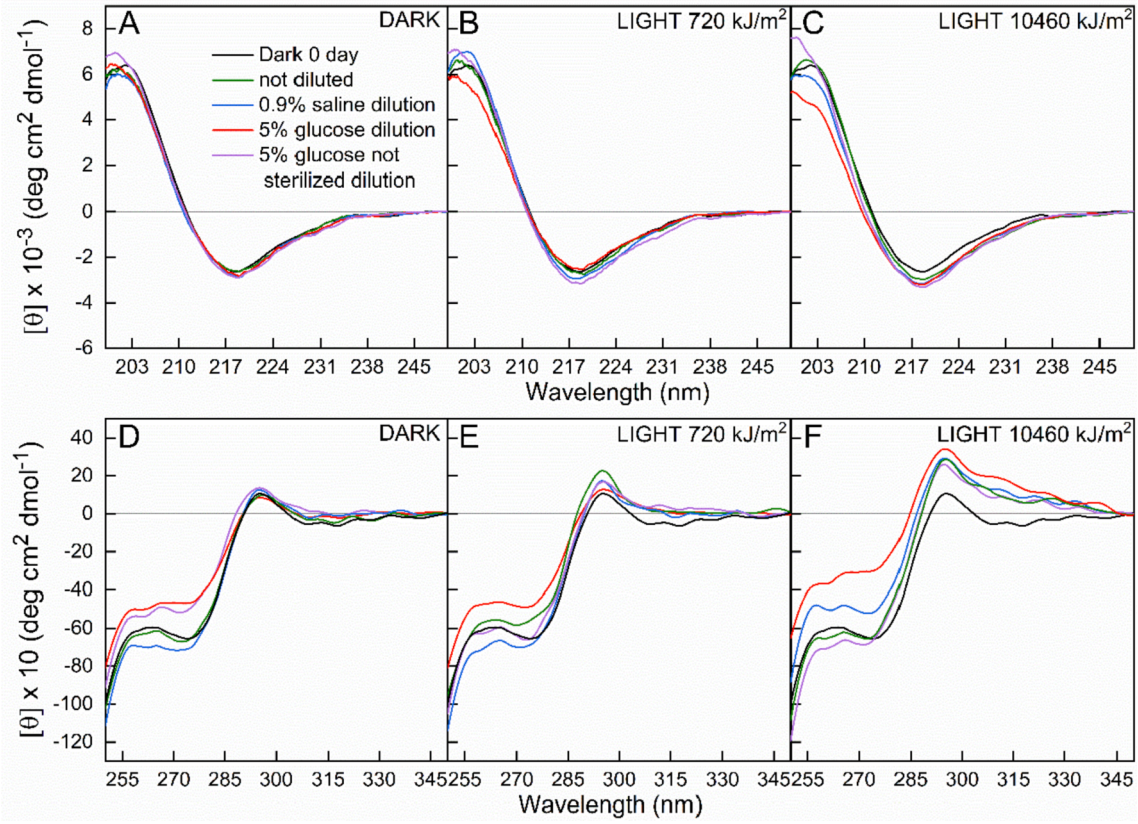

Fig. 4. Characterization of the effects of light exposure on the structure of Ipilimumab monitored by far UV (A-C) and near UV (D-F) circular dichroism. The measurements were conducted after exposure of the protein samples under 720 and 10460 kJ/m^2 of artificial sunlight. The samples were measured after 0.9% saline dilution (light blue), 5% glucose dilution (red), 5% not sterile glucose dilution (purple) in comparison to the not diluted sample (green) and the dark control (black). All samples were analyzed by using the same concentration of 0.1 mg/mL for the far-UV CD and 0.5 mg/mL in the near-UV CD. (For interpretation of the references to color in this figure legend, the reader is referred to the web version of this article.)

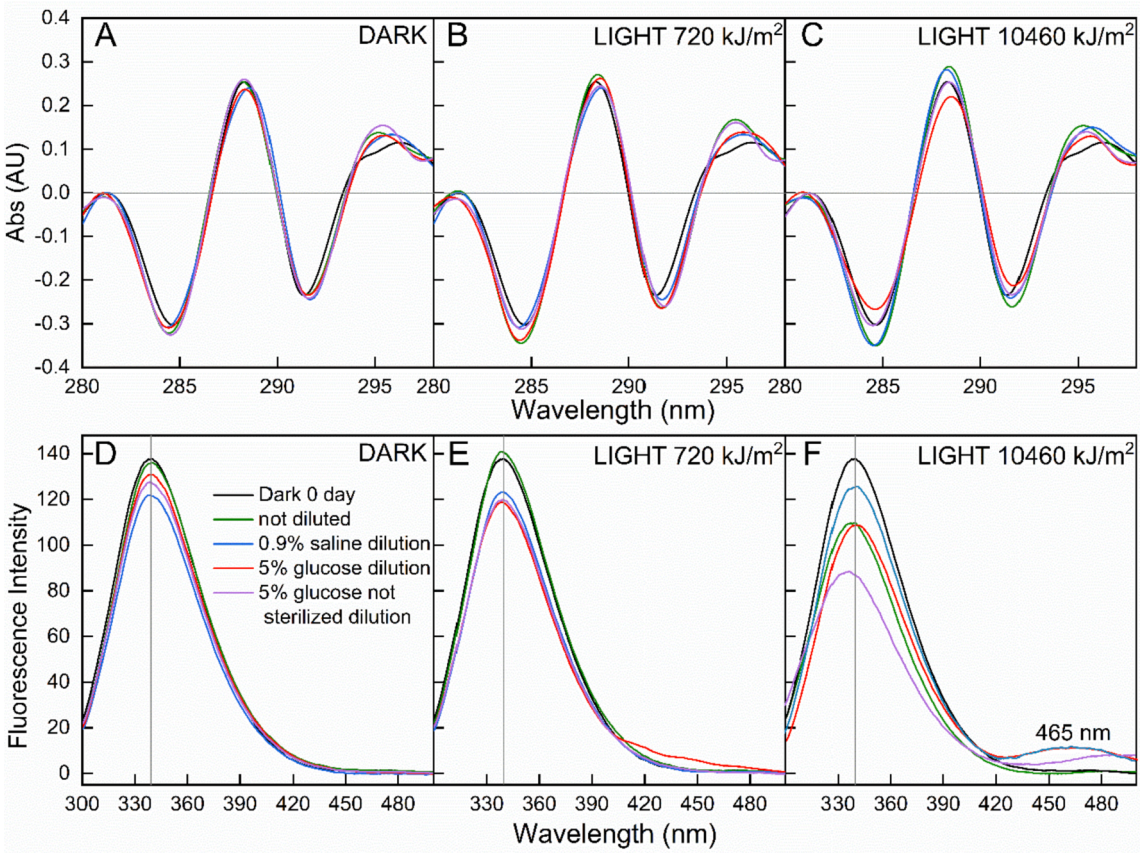

Fig. 5. Characterization of the effects of the light exposure on the structure of Ipilimumab monitored by UV second derivative (A-C) and intrinsic fluorescence spectroscopy (D-F). The measurements were conducted after exposure of the protein samples under 720 and 10460 kJ/m^2 of artificial sunlight. The samples were measured after 0.9% saline dilution (light blue), 5% glucose dilution (red), 5% not sterile glucose dilution (purple) in comparison to the not diluted one (green) and the dark control (black). Fluorescence emission spectra were collected after excitation at 280 nm. Experimental details are reported in Methods section. (For interpretation of the references to color in this figure legend, the reader is referred to the web version of this article.)

species was evident at intense light doses and the elution volume of the monomer was shifted to shorter values, both aggregation and chemical modification of the mAb could have occurred. However, the aggregation of Ipilimumab took place also in the non-diluted formulation, indicating that the ingredients did not protect the drug from photodegradation (Fig. 3C). Table 1 reports the physical parameters of the mAb before and after the two irradiation doses; the elution volume (mL) in SEC and the diameter (nm) measured by DLS. According to SEC profiles, Ipilimumab diameters increased from 9.65 to 11.23 nm after 720 kJ/m^2 of artificial sunlight. Under the second light exposure, the samples appeared populated by different species as evidenced by the change in the elution volume and shape of the peaks. Interestingly, the greatest effect in both light conditions was observed in the 5% sterile glucose solution (Fig. 3E, F, red line). The obtained results were then confirmed by electrophoretic techniques. The native-PAGE of Ipilimumab irradiated with 720 kJ/m^2 showed the presence of aggregates only in the diluted 5% glucose solution sample (well 4) (Fig. 3G, left). For the other diluted samples and the non-irradiated (dark) samples, it was possible to visualize the presence of the monomer with a MW of ~ 150 kDa only. By SDS-PAGE analysis of Ipilimumab irradiated with 720 kJ/m^2 (Fig. 3G, right), all the samples showed the two characteristic bands, at ~ 50 kDa for the heavy chain and at ~ 25 kDa for the light chain. The irradiation of Ipilimumab with 10460 kJ/m^2 showed the presence of aggregates in all the irradiated samples (2, 3, 4, 5 wells), especially in the 5% glucose and 0.9% saline diluted solutions (Fig. 3H, left). It was possible to detect other bands with higher MW only in the sample diluted with 5% sterile glucose, demonstrating the highest vulnerability of the mAb in this solution. The SDS-PAGE analysis of Ipilimumab before and after irradiation with 10460 kJ/m^2 is shown in Fig. 3H, right. The lanes relative to the dark samples contained the two characteristic bands, while the irradiated ones (wells 2, 3, 4, and 5) showed high molecular weight species and other species with an intermediate molecular weight between light and heavy chains.

To investigate changes in the conformation of the mAb, CD measurements in the far-UV region (250–195 nm) were performed (Fig. 4A-C). After irradiation with 720 kJ/m^2 (B) and with 10460 kJ/m^2 (C), Ipilimumab maintained its typical β-sheets structure, with the characteristic negative band at 218 nm and the positive one at 200 nm. The tertiary structure was studied using near-UV CD spectroscopy (Fig. 4D-F). In panel E, during the irradiation with 720 kJ/m^2, the tertiary structure of Ipilimumab was nearly maintained compared to the dark (panel D). A slight deviation from the main trend could be observed only in samples irradiated under 10460 kJ/m^2 (Fig. 4F). To better explore the chemical environment of the chromophores, the second-derivative UV spectra were calculated to gain information about the tertiary structure of mAb under the light stress (Fig. 5). These data were obtained using the samples irradiated with 720 kJ/m^2 (B) and with 10460 kJ/m^2 (C) and compared to the dark control (A). The tertiary structure was not significantly altered, but some changes in intensity and position of the main minima (284, 288, 292 and 295 nm) were visible in the diluted sample with 5% sterile glucose solution.

Fig. 5E reports the intrinsic fluorescence of Ipilimumab after the irradiation with 720 kJ/m^2. The excitation at 280 nm showed the maximal emission wavelength at ~ 339 nm, suggesting that the mAb tertiary structure remained substantially unchanged as in the dark (D). Instead, the intensity of emission spectra of the samples diluted with 5%

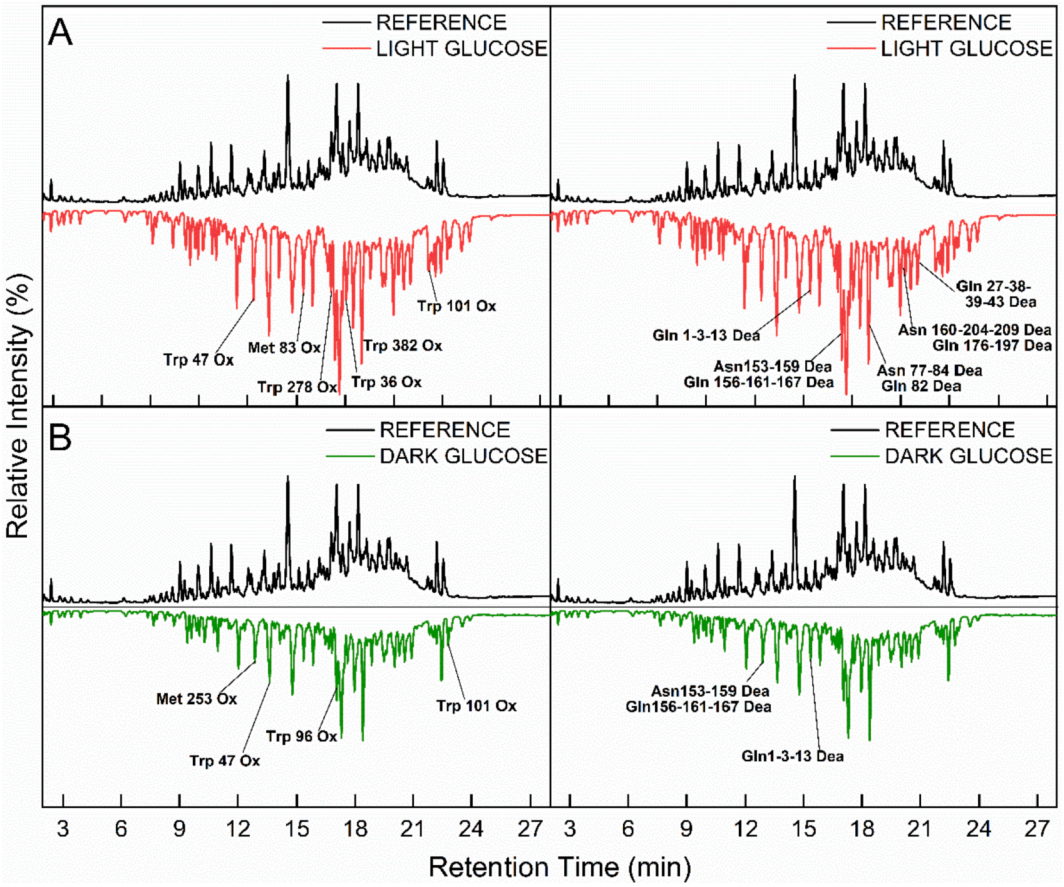

Fig. 6. Fingerprinting analysis by trypsin of Ipilimumab after reduction of disulfide bonds and carboxymethylation of free cysteine residues by LC-MS/MS. A. Chromatograms of the irradiated 5% glucose diluted sample (red) in comparison to the reference one (black). B. Chromatograms of the 5% glucose diluted sample (green) in comparison to the same reference (black). The exposure to light was performed with 720 kJ/m^2 of artificial sunlight. The numbers close to the peaks refer to the modified residues, oxidized (left) and deamidated (right), as found by MS analysis (Tables 2-4). (For interpretation of the references to color in this figure legend, the reader is referred to the web version of this article.)

sterile glucose or saline solution decreased after exposure with 10460 kJ/m^2 light, and a new band was observed at 465 nm (Fig. 5F). Since 5% sterile glucose dilution presented the greatest contribution to the protein aggregation and structure alteration, the fingerprinting analysis by trypsin (Fig. 6) was performed before (A) and after (B) irradiation (720 kJ/m^2) and compared with the non-diluted sample as a control (upper panels). The proteolytic mixtures were analyzed by LC-MS/MS to verify the presence of modifications at the side chains of residues in the polypeptide chain. Collected data were processed by MassLynxTM mass spectrometry software. Tryptic peptides were matched with their calculated molecular mass, obtaining a good coverage with the mAb sequence (Tables 2-4). Table 3 reports the list of peptide species coming from Ipilimumab diluted in 5% sterile glucose solution and found after the irradiation, while in Table 4 the peptide species obtained from the non-irradiated but in the same buffer sample were reported as a control. The peptide map for the dark sample showed a certain number of oxidations at the level of Trp and Met residues compared to the non-diluted sample. In the case of the irradiated sample (720 kJ/m^2) (Fig. 6B), the oxidation contribution was more evident. The oxidation was especially observed on Trp 36, 47, 101, 278, and 382 (light chain), Met 83 and 253 (heavy chain). It was previously reported that Trp is the most involved residue in the photodegradation pathways of proteins even though it is present in relatively low amount [22]. Moreover, the presence of deamidated peptides at the level of Asn and Gln in the irradiated samples was detected. Several deamidated species were also found in the dark control suggesting that this chemical modification was not correlated to light exposure, but to the dilution effect.

3.3. Dilution

The leaflet of most commercial therapeutic mAbs recommends the use of a diluted formulation for patient administration stored at 4° C in the dark and not exceeding 8–24 h. This short-term stability is probably recommended to avoid bacterial contamination during the centralized preparation in the hospital pharmacies. Yervoy® stability is reported to last 24 h at both room temperature and 4° C. In this work, the stability of the sodium chloride diluted formulation of Ipilimumab was tested up to 30 days at a concentration of 1 mg/mL, which is the highest dilution approved by the pharmaceutical manufacturer. After dilution, the samples were stored in the refrigerator prior to analysis.

The diluted Ipilimumab samples (1 mg/mL) were analyzed by SEC (Fig. 7A). Two days after dilution, the development of large aggregates, which eluted at 1.6–2.1 mL, was detected. Notably, these aggregates appeared different in size from those formed under light. However, the extent of aggregation did not increase during prolonged incubation unlike the light stressor under increased doses. The percentage of soluble

Table 2
Retention Time (RT) in RP-HPLC (Fig. 6) and molecular masses of peptide species found after the digestion of Ipilimumab (reference) with trypsin. Carboxymethylated Cys residues are indicated in red and the peptide with a red star. In grey background, the fragments derived from the light (L) chain are listed, whereas the fragments from the heavy (H) chain are listed in the white background.

RP-HPLC RT (min)	*Molecular Mass (Da)*		*Peptide species*	*Sequence*
	Found	*Calculated*		
3.4	346.23 ± 0.5	346.19	L 144-146	EAK
6.14	624.28 ± 0.37	624.28	L 185-189	ADYEK
7.7	522.26 ± 0.29	522.26	L 209-212	SFNR
9.1	706.35 ± 0.41	706.34	L 19-24	ATLSCR*
9.3	487.31 ± 0.21	487.30	L 105-108	VEIK
10.4	728.40 ± 0.32	728.38	L 56-62	ATGIPDR
11.2	559.32 ± 0.05	559.31	L 147-150	VQWK
11.7	2132.98 ± 0.17	2134.96	L 151-170	VDNALQSGNSQESVTEQDSK
13.1	1038.47 ± 0.5	1038.59	L 47-55	LLIYGAFSR
13.4	1874.92 ± 0.13	1874.92	L 192-208	VYACEVTHQGLSSPVTK*
14.1	2408.17 ± 0.5	2408.19	L 25-46	ASQSVGSSYLAWYQQKPGQAPR
17.2	1631.78 ± 0.33	1631.78	L 63-78	FSGSGSGTDFTLTISR
17.4	1883.01 ± 0.54	1883.00	L 1-18	EIVLTQSPGTLSLSPGER
18.5	1944.92 ± 0.5	1945.02	L 110-127	TVAAPSVFIFPPSDEQLK
20.0	1501.88 ± 0.50	1501.75	L 171-184	DSTYSLSSTLTLSK
22.1	1796.88 ± 0.56	1796.89	L 128-143	SGTASVVCLLNNFYPR*
22.5	3001.4 ± 2.75	3000.33	L 79-104	LEPEDFAVYYCQQYGSSPWTFGQGTK
2.4	499.27 ± 0.3	499.28	H 39-43	QAPGK
2.4	456.24 ± 0.18	456.24	H 342-345	GQPR
2.8	438.21 ± 0.57	438.21	H 319-321	EYK
2.9	471.27 ± 0.53	471.27	H 216-219	VEPK
3.4	447.27 ± 0.36	447.27	H 336-339	TISK
3.9	374.23 ± 0.48	374.23	H 17-19	SLR
8.0	604.3 ± 0.61	604.31	H 357-361	DELTK
8.1	500.26 ± 0.50	500.31	H 290-293	TKPR
8.4	446.26 ± 0.5	446.25	H 324-327	VSNK
9.6	462.26 ± 0.50	462.21	H 73-76	DNSK

(*continued on next page*)

Table 2 (*continued*)

9.7	360.2 ± 0.69	360.2	H 212-214	VDK
9.7	574.33 ± 0.17	574.33	H 411-415	LTVDK
10.8	844.39 ± 0.41	844.40	H 59-65	YYADSVK
11.4	787.44 ± 0.5	787.44	H 441-448	SLSLSPGK
12.5	1285.59 ± 0.5	1285.67	H 346-356	EPQVYTLPPSR
12.6	622.34 ± 0.06	622.34	H 68-72	FTISR
12.7	508.28 ± 0.5	508.20	H 220-223	SCDK*
13.3	837.5 ± 1.04	837.5	H 328-335	ALPAPIEK
13.4	1872.94 ± 0.5	1872.91	H 394-410	TTPPVLDSDGSFFLYSK
13.9	834.42 ± 0.26	834.43	H 250-256	DTLMISR
14.4	1608.85 ± 0.6	1608.86	H 1-16	QVQLVESGGGVVQPGR
15.6	1320.66 ± 0.02	1320.67	H 135-148	STSGGTAALGCLVK*
16.2	1807.9 ± 0.5	1807	H 303-318	VVSVLTVLHQDWLNGK
16.4	1274.5 ± 0.50	1274.56	H 88-98	AEDTAIYYCAR
16.6	1160.62 ± 0.09	1160.62	H 362-371	NQVSLTCLVK*
16.8	1351.66 ± 2.58	1351.69	H 77-87	NTLYLQMNSLR
16.8	2138.02 ± 0.01	2138.02	H 257-275	TPEVTCVVVDVSHEDPEVK*
16.9	1188.65 ± 0.50	1188.50	H 294-302	EEQYNSTYR
17.0	1185.64 ± 0.08	1185.64	H 123-134	GPSVFPLAPSSK
17.1	1676.79 ± 0.08	1676.79	H 276-289	FNWYVDGVEVHNAK
18.4	2729.20 ± 0.5	2729.41	H 224-249	THTCPPCPAPELLGGPSVFLFPPKPK
19.3	2543.12 ± 0.09	2543.12	H 372-393	GFYPSDIAVEWESNGQPENNYK
20.1	1741.83 ± 0.08	1741.83	H 44-58	GLEWVTFISYDGNNK
20.4	2800.25 ± 0.51	2800.26	H 418-440	WQQGNVFSCSVMHEALHNHYTQK*
22.1	2207.01 ± 0.72	2206.99	H 20-38	LSCAASGFTFSSYTMHWVR*
23.1	6712.27 ± 0.54	6712.31	H 149-211	DYFPEPVTVSWNSGALTSGVHTFPA VLQSSGLYSLSSVVTVPSSSLGTQT YICNVNHKPSNTK*
23.3	2557.24 ± 0.4	2557.25	H 99-122	TGWLGPFDYWGQGTLVTVSSASTK

aggregates was 2.4% in all samples from 2 to 30 days of incubation. Only in the last sample (30 days) 3% of the soluble protein was lost. SDS-PAGE (inset) showed the presence of the two characteristic bands in all the lanes, while after 30 day-dilution the protein appeared partially degraded and species with molecular weight between light and heavy chains were visible. UV–Vis absorption measurements of diluted Ipilimumab confirmed the presence of aggregates that induced light scattering above 320 nm. After five day-dilution there was a slight increment of absorption at about 400 nm (Fig. 7B). In the inset, the second-derivative UV spectra showed a minimal shift of the main signals at 285, 288, 292 and 295 nm. The 0.9% saline diluted sample was digested by trypsin after 10 days (blue line) and the tryptic map was compared with the chromatogram of the tryptic digest of the freshly reconstituted mAb (black line) (Fig. 7C). Oxidation of Trp and Met residues was detected. Table 5 reports the mass analysis of the tryptic fragments, and those containing the modifications are highlighted. The oxidation was especially observed on Trp 97, 149 (light chain), Met 83, 253 and Trp 47, 101, 278, 314 (heavy chain). Moreover, the presence of deamidated

Table 3
RT in RP-HPLC (Fig. 6A) and molecular masses of peptide species found after the tryptic digestion of Ipilimumab diluted in 5% sterile glucose solution after the irradiation with 720 kJ/m^2. Carboxymethylated Cys residues are indicated with a red star. In grey background, the fragments derived from the light (L) chain are listed, whereas the fragments from the heavy (H) chain are listed in the white background. Oxidized amino acids are indicated with a blue star. Deamidated amino acids are indicated with an orange star.

RP-HPLC RT (min)	*Molecular Mass (Da)*		*Peptide species*	*Sequence*
	Found	*Calculated*		
3.4	346.23 ± 0.5	346.19	L 144-146	EAK
6.3	624.30 ± 0.06	624.28	L 185-189	ADYEK
7.8	522.28 ± 0.13	522.26	L 209-212	SFNR
9.4	706.35 ± 0.08	706.34	L 19-24	ATLSCR*
9.6	487.32 ± 0.23	487.30	L 105-108	VEIK
10.8	728.40 ± 0.05	728.38	L 56-62	ATGIPDR
14.3	1875.90 ± 0.01	1875.90	L 192-208	VYACEVTHQGLSSPVTK**
15.3	592.29 ± 0.15	592.29	L 147-150	VQWK**
17.0	2139.82 ± 0.28	2139.88	L 151-170	VDNALQSGNSQESVTEQDSK*
17.1	3238.33 ± 0.68	3238.35	L 79-104	LEPEDFAVYYCQQYGSSPWTFGQG TK *
17.4	1631.79 ± 0.06	1631.78	L 63-78	FSGSGSGTDFTLTISR
17.5	1501.76 ± 0.57	1501.75	L 171-184	DSTYSLSSTLTLSK
17.7	1798.87 ± 0.03	1798.86	L 128-143	SGTASVVCLLNNFYPR**
17.7	1883.01 ± 0.50	1883.00	L 1-18	EIVLTQSPGTLSLSPGER
18.8	1038.60 ± 0.45	1038.59	L 47-55	LLIYGAFSR
20.6	1945.02 ± 0.58	1945.02	L 110-127	TVAAPSVFIFPPSDEQLK
20.8	2444.16 ± 0.04	2444.11	L 25-46	ASQSVGSSYLAWYQQKPGQAPR**
2.8	438.22 ± 0.39	438.21	H 319-321	EYK
2.9	471.28 ± 0.23	471.27	H 216-219	VEPK
3.1	447.28 ± 0.07	447.27	H 336-339	TISK
3.9	374.23 ± 0.35	374.23	H 17-19	SLR
8.2	604.32 ± 0.15	604.31	H 357-361	DELTK
8.3	500.26 ± 0.50	500.31	H 290-293	TKPR
8.3	500.26 ± 0.05	500.26	H 39-43	QAPGK *
9.8	457.23 ± 0.01	457.23	H 342-345	GQPR *

(*continued on next page*)

Table 3 (*continued*)

9.9	462.26 ± 0.50	462.21	H 73-76	DNSK
10.0	360.21 ± 0.39	360.2	H 212-214	VDK
10.1	574.35± 0.19	574.33	H 411-415	LTVDK
10.1	1710.77 ± 0.11	1710.75	H 276-289	FNWYVDGVEVHNAK**
11.1	844.41 ± 0.02	844.40	H 59-65	YYADSVK
11.6	447.33 ± 0.41	447.23	H 324-327	VSNK *
11.8	787.45 ± 0.77	787.44	H 441-448	SLSLSPGK
12.9	622.36 ± 0.16	622.34	H 68-72	FTISR
13.0	508.28 ± 0.5	508.20	H 220-223	SCDK *
13.6	837.51 ± 0.04	837.5	H 328-335	ALPAPIEK
14.0	446.26 ± 0.5	446.25	H 324-327	VSNK
14.2	1775.23 ± 0.14	1775.79	H 44-58	GLEWVTFISYDGNNK**
14.3	866.41 ± 0.07	866.42	H 250-256	DTLMISR *
14.7	1190.51 ± 0.22	1190.47	H 294-302	EEQYNSTYR *
15.5	1611.92± 0.06	1611.81	H 1-16	QVQLVESGGGVVQPGR *
15.5	1286.75 ± 0.14	1286.65	H 346-356	EPQVYTLPPSR *
15.9	1320.67 ± 0.02	1320.67	H 135-148	STSGGTAALGCLVK *
16.5	1274.5 ± 0.50	1274.56	H 88-98	AEDTAIYYCAR
16.6	2800.24 ± 0.57	2800.26	H 418-440	WQQGNVFSCSVMHEALHNHYTQK *
16.9	2622.24 ± 0.09	2622.21	H 99-122	TGWLGPFDYWGQGTLVTVSSASTK **
17.1	2138.02 ± 0.18	2138.02	H 257-275	TPEVTCVVVDVSHEDPEVK *
17.2	1185.64 ± 0.15	1185.64	H 123-134	GPSVFPLAPSSK
17.9	1162.57 ± 0.11	1162.59	H 362-371	NQVSLTCLVK **
18.3	1386.64 ± 0.54	1386.63	H 77-87	NTLYLQMNSLR **
18.6	2729.17 ± 0.50	2729.41	H 224-249	THTCPPCPAPELLGGPSVFLFPPKPK
19.5	2543.1 ± 0.50	2543.12	H 372-393	GFYPSDIAVEWESNGQPENNYK
20.0	2206.98 ± 0.52	2206.99	H 20-38	LSCAASGFTFSSYTMHWVR *
20.3	1872.91 ± 0.50	1872.91	H 394-410	TTPPVLDSDGSFFLYSK
20.9	1840.90 ± 0.29	1840.96	H 303-318	VVSVLTVLHQDWLNGK **
23.3	6750.17 ± 0.05	6750.20	H 149-211	DYFPEPVTVSWNSGALTSGVHTFPA VLQSSGLYSLSSVVTVPSSSLGTQTY ICNVNHKPSNTK ***

peptides was detected at the level of Asn and Gln, especially on Asn 277, 287, 385, 390 and Gln 1, 3, 13, 110, 387.

The intrinsic fluorescence was measured, by exciting the samples at 280 nm, considering the contribution of Trp and Tyr residues. Fluorescent emission spectra showed the characteristic maximal emission wavelength at ~ 339 nm, until 2 days of dilution (Fig. 8A). The reduction of the Trp signal and fingerprinting analysis suggest an oxidative process of the protein in the formulation. To maximize this effect, the formulation was further diluted up to 0.1 mg/mL with 0.9% saline buffer. In this case, higher aggregation was observed by SEC (not shown). After five days from sample dilution, a fluorescent band at 465 nm, already observed under light exposure, was visible (Fig. 8B). The increase of this band was concomitant with the reduced intensity of the signal at 339 nm, likewise in the presence of light. To confirm protein

Table 4
RT in RP-HPLC (Fig. 6B) and molecular masses of peptide species found after the tryptic digestion of Ipilimumab diluted in 5% sterile glucose solution as dark control sample. Carboxymethylated Cys residues are indicated with a red star. In grey background, the fragments derived from the light chain (L) are listed, whereas the fragments from the heavy chain (H) are listed in the white background. Oxidized amino acids are indicated with a blue star. Deamidated amino acids are indicated with an orange star.

RP-HPLC RT (min)	*Molecular Mass (Da)*		*Peptide species*	*Sequence*
	Found	*Calculated*		
3.4	346.23 ± 0.5	346.19	L 144-146	EAK
6.2	624.30 ± 0.06	624.28	L 185-189	ADYEK
7.8	522.28 ± 0.17	522.26	L 209-212	SFNR
9.3	706.34 ± 0.04	706.34	L 19-24	ATLSCR*
9.6	487.32 ± 0.39	487.30	L 105-108	VEIK
10.7	728.40 ± 0.14	728.38	L 56-62	ATGIPDR
11.5	559.32 ± 0.25	559.31	L 147-150	VQWK
12.8	2139.91 ± 0.02	2139.88	L 151-170	VDNALQSGNSQESVTEQDSK*
14.3	1875.90 ± 0.01	1875.90	L 192-208	VYACEVTHQGLSSPVTK**
17.3	1631.80 ± 0.02	1631.78	L 63-78	FSGSGSGTDFTLTISR
17.1	1501.76 ± 0.67	1501.75	L 171-184	DSTYSLSSTLTLSK
17.4	1884.02 ± 0.02	1883.98	L 1-18	EIVLTQSPGTLSLSPGER
17.6	2428.07 ± 0.20	2428.12	L 25-46	ASQSVGSSYLAWYQQKPGQAPR*
17.7	1798.87 ± 0.06	1798.86	L 128-143	SGTASVVCLLNNFYPR*
18.8	1038.58 ± 0.2	1038.59	L 47-55	LLIYGAFSR
18.5	1945.00 ± 0.6	1945.02	L 110-127	TVAAPSVFIFPPSDEQLK
21.4	3057.32 ± 0.87	3057.35	L 79-104	LEPEDFAVYYCQQYGSSPWTFGQGTK*
2.8	438.22 ± 0.25	438.21	H 319-321	EYK
2.8	471.28 ± 0.02	471.27	H 216-219	VEPK
3.1	447.28 ± 0.02	447.27	H 336-339	TISK
3.9	374.23 ± 0.19	374.23	H 17-19	SLR
8.2	604.32 ± 0.05	604.31	H 357-361	DELTK
8.23	500.26 ± 0.50	500.31	H 290-293	TKPR
8.3	500.26± 0.05	500.26	H 39-43	QAPGK*
10	360.21 ± 0.25	360.2	H 212-214	VDK
10	574.36 ± 0.44	574.33	H 411-415	LTVDK

(*continued on next page*)

Table 4 (*continued*)

10.1	1710.77± 0.09	1710.75	H 276-289	FNWYVDGVEVHNAK**
11.1	844.42 ± 0.02	844.40	H 59-65	YYADSVK
11.2	463.20 ± 0.25	463.19	H 73-76	DNSK*
11.6	447.23 ± 0.04	447.23	H 324-327	VSNK*
11.7	787.46 ± 0.67	787.44	H 441-448	SLSLSPGK
12.8	622.36 ± 0.32	622.34	H 68-72	FTISR
12.9	508.28 ± 0.5	508.20	H 220-223	SCDK*
12.9	850.42 ± 0.09	850.42	H 250-256	DTLMISR*
13.5	837.52 ± 0.54	837.5	H 328-335	ALPAPIEK
14.1	1331.57 ± 0.52	1331.58	H 88-98	AEDTAIYYCAR*
14.2	1775.80 ± 0.04	1775.79	H 44-58	GLEWVTFISYDGNNK***
14.8	457.22 ± 0.29	457.23	H 342-345	GQPR*
14.8	1190.51 ± 0.29	1190.47	H 294-302	EEQYNSTYR*
15.3	1367.68 ± 0.54	1367.69	H 77-87	NTLYLQMNSLR*
15.3	1806.98 ± 1.32	1807	H 303-318	VVSVLTVLHQDWLNGK
15.5	1611.82± 0.04	1611.81	H 1-16	QVQLVESGGGVVQPGR*
15.9	2729.31 ± 0.5	2729.41	H 224-249	THTCPPCPAPELLGGPSVFLFPPKPK
16.6	2800.25 ± 0.37	2800.26	H 418-440	WQQGNVFSCSVMHEALHNHYTQK*
16.9	1285.61 ± 0.5	1285.67	H 346-356	EPQVYTLPPSR
17.0	2622.23 ± 0.08	2622.21	H 99-122	TGWLGPFDYWGQGTLVTVSSASTK**
17.1	2081.05 ± 0.36	2138.02	H 257-275	TPEVTCVVVDVSHEDPEVK*
17.1	1185.64 ± 0.59	1185.64	H 123-134	GPSVFPLAPSSK
17.2	1263.65 ± 0.65	1263.65	H 135-148	STSGGTAALGCLVK
18.4	2559.12 ± 0.09	2559.12	H 372-393	GFYPSDIAVEWESNGQPENNYK*
18.6	1103.62 ± 0.34	1103.60	H 362-371	NQVSLTCLVK
20	2206.98 ± 0.38	2206.99	H 20-38	LSCAASGFTFSSYTMHWVR*
20.2	1872.92 ± 0.40	1872.91	H 394-410	TTPPVLDSDGSFFLYSK
23.3	6712.27 ± 0.52	6712.31	H 149-211	DYFPEPVTVSWNSGALTSGVHTFPAVLQSSGLYSLSSVVTVPSSSLGTQTYICNVNHKPSNTK*

oxidation phenomena, the intrinsic fluorescence of Ipilimumab upon dilution was analyzed in the presence of catalase (1:1 catalase/hydrogen peroxide). Catalase acts as a scavenger to remove hydrogen peroxide and prevents oxidation. The experiment was also conducted in the presence of mineral oil stratified on the samples to avoid contact with air. The formation of the band at 465 nm considerably decreased in favor of the signal at 339 nm in the presence of catalase or completely inhibited in the presence of oil (Fig. 8 C, D). These data confirm that the emission signal at 465 nm was derived from an oxidative mechanism inducing the formation of new species.

3.4. Stressed Ipilimumab effect on cell viability

The toxicity of stressed Ipilimumab by light was investigated on human cerebral microvascular endothelial (HBEC-5i) and melanoma (SK-MEL-28) cells. The cells were exposed for 24 and 72 h to Ipilimumab samples (0.67 mM, left panels and 3.36 mM, right panels) irradiated with 720 and 10460 kJ/m^2 of artificial sunlight to assay their

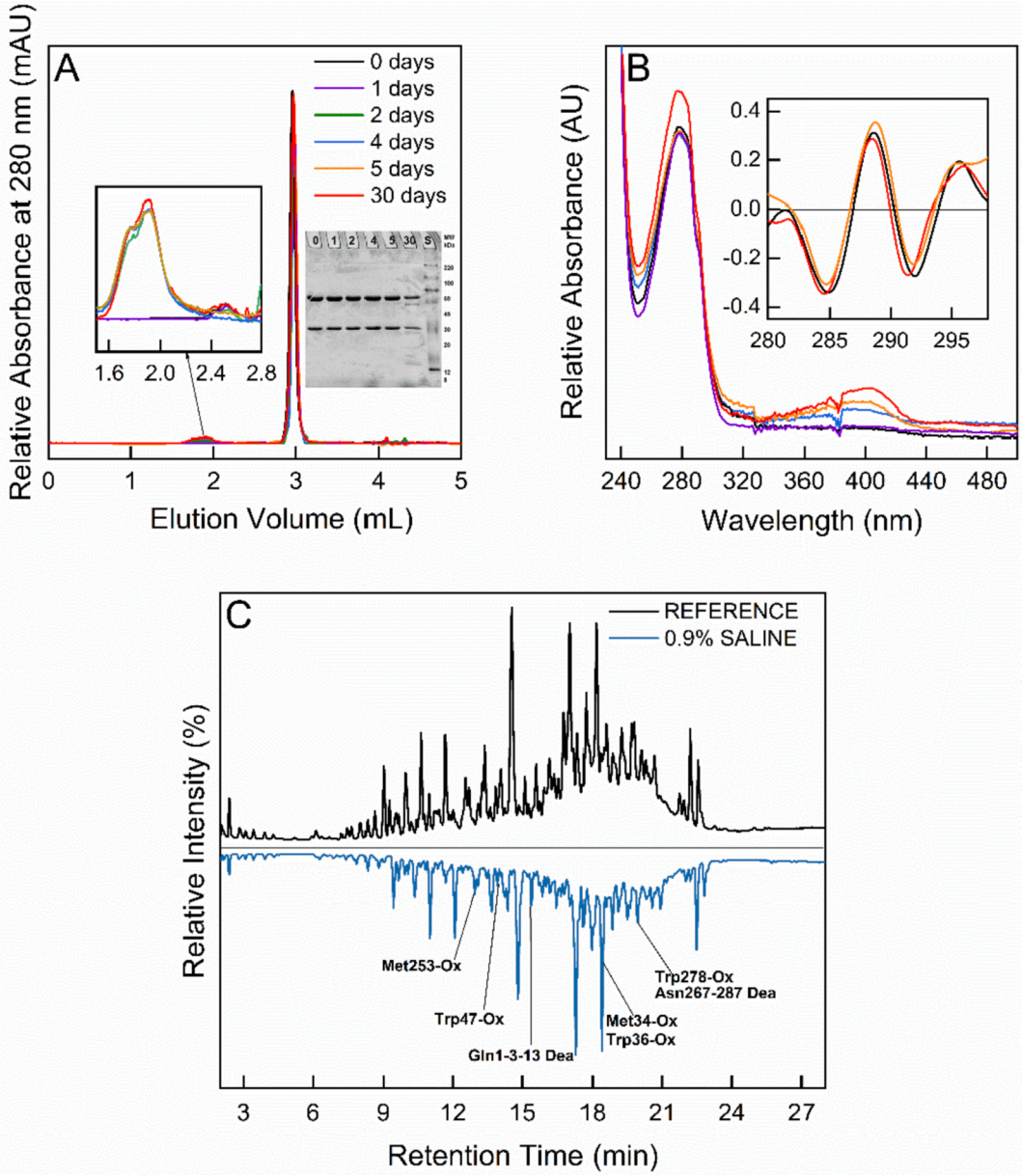

Fig. 7. Characterization of the effects of the saline dilution on the stability of Ipilimumab monitored by SEC (A), UV–Vis measurements (B) and LC-MS/MS after tryptic digestion of reduced and carboxymethylated Ipilimumab after dilution in 0.9 % saline solution for 10 days (blue) and non-diluted (black) (C). The numbers close to the peaks refer to the oxidized and deamidated residues, as found by MS analysis (Table 5). Insets in A report the zoomed SEC chromatogram (from 1.5 to 2.8 mL, left) and the SDS-PAGE analysis (right) of aliquots of the samples collected at the given time points. Lane 1–6, mAb after 0, 1, 2, 4, 5 and 30 days of incubation; lane 7, MW standard proteins (S). Inset in B reports the second derivative of UV profiles. (For interpretation of the references to color in this figure legend, the reader is referred to the web version of this article.)

cytotoxicity (Fig. 9). The cell viability slightly decreased only when the cell-treatment was performed with a high concentration of the irradiated samples (3.36 mM). In particular, HBEC-5i cells exhibited a moderate sensitivity at 24 h of treatment, while SK-MEL appeared vulnerable when the treatment was prolonged to 72 h. Overall, these preliminary results suggest a low toxicity of the stressed mAb.

4. Discussion

The real-life handling of protein drugs can expose this class of molecules to a variety of stressors (e.g., shaking, humidity, light, dilution) that could generate structural protein perturbation, jeopardizing their stability and, therefore, biological activity. Aggregation, chemical modification, and conformational alteration with loss of the original secondary and tertiary structure could occur, but the extent of these processes is strongly molecule dependent. Therefore, mAbs should be evaluated individually, and stability parameters applied in accordance. Real-life stability of therapeutic drugs guarantees patient safety. Indeed, altered proteins could be less effective and/or responsible for immunogenicity.

This work investigates the biophysical-chemical behavior of the mAb Ipilimumab when exposed to multiple stressors encountered during its real-life steps, i.e., transportation, storage, preparation/dilution, distribution, administration. Moreover, accidental falls and temperature fluctuations could occur affecting drug integrity. Bardo-Brouard et al. [37] have documented the stability of Ipilimumab at 4 and 25 °C, over one month after opening the drug vial. In our work, we have demonstrated that Ipilimumab was stable for up to 45 days, even under forced

Table 5
RT in RP-HPLC (Fig. 7C) and molecular masses of peptide species found after the tryptic digestion of Ipilimumab diluted in 0.9% sterile saline solution. Carboxymethylated Cys residues are indicated with a red star. In grey background, the fragments derived from the light (L) chain are listed, whereas the fragments from the heavy (H) chain are listed in the white background. Oxidized amino acids are indicated with a blue star. Deamidated amino acids are indicated with an orange star.

RP-HPLC RT (min)	*Molecular Mass (Da)*		*Peptide species*	*Sequence*
	Found	*Calculated*		
3.4	346.23 ± 0.5	346.19	L 144-146	EAK
6.2	624.28 ± 0.39	624.28	L 185-189	ADYEK
7.8	522.26 ± 0.28	522.26	L 209-212	SFNR
9.2	592.27 ± 0.03	592.29	L 147-150	VQWK**
9.3	706.35 ± 0.41	706.34	L 19-24	ATLSCR*
9.6	487.31 ± 0.21	487.30	L 105-108	VEIK
10.4	728.40 ± 0.32	728.38	L 56-62	ATGIPDR
11.7	2132.98 ± 0.20	2134.96	L 151-170	VDNALQSGNSQESVTEQDSK
13.1	1038.47 ± 0.5	1038.59	L 47-55	LLIYGAFSR
13.7	1874.92 ± 0.20	1874.92	L 192-208	VYACEVTHQGLSSPVTK*
14.7	1944.88 ± 0.5	1945.02	L 110-127	TVAAPSVFIFPPSDEQLK
17.3	1631.78 ± 0.33	1631.78	L 63-78	FSGSGSGTDFTLTISR
17.4	1883.01 ± 0.54	1883.00	L 1-18	EIVLTQSPGTLSLSPGER
17.7	1798.86 ± 0.02	1798.86	L 128-143	SGTASVVCLLNNFYPR*
20.2	3092.19 ± 0.42	3092.29	L 79-104	LEPEDFAVYYCQQYGSSPWTFG QGTK****
2.8	438.22 ± 0.28	438.21	H 319-321	EYK
2.8	471.28 ± 0.47	471.27	H 216-219	VEPK
3.1	447.27 ± 0.03	447.27	H 336-339	TISK
3.9	374.23 ± 0.41	374.23	H 17-19	SLR
8.2	604.30 ± 0.09	604.31	H 357-361	DELTK
8.3	499.27 ± 0.30	499.28	H 39-43	QAPGK
10	360.20 ± 0.06	360.2	H 212-214	VDK
10	574.33 ± 0.51	574.33	H 411-415	LTVDK
11.1	844.40 ± 0.39	844.40	H 59-65	YYADSVK
11.2	463.19 ± 0.19	463.19	H 73-76	DNSK*
11.6	447.22 ± 0.07	447.23	H 324-327	VSNK*
11.7	787.44 ± 0.04	787.44	H 441-448	SLSLSPGK

(*continued on next page*)

Table 5 (*continued*)

12.8	622.34 ± 0.62	622.34	H 68-72	FTISR
12.9	508.21 ± 0.06	508.20	H 220-223	SCDK*
13.3	866.41 ± 0.13	866.42	H 250-256	DTLMISR**
13.5	837.5 ± 0.33	837.5	H 328-335	ALPAPIEK
14.8	456.25 ± 0.03	456.24	H 342-345	GQPR
15.4	1367.60 ± 0.50	1367.69	H 77-87	NTLYLQMNSLR*
15.5	1611.77 ± 0.23	1611.81	H 1-16	QVQLVESGGGVVQPGR*
15.9	1320.66 ± 0.20	1320.67	H 135-148	STSGGTAALGCLVK*
16.7	1775.83 ± 0.23	1775.79	H 44-58	GLEWVTFISYDGNNK***
16.8	1286.63 ± 0.10	1286.63	H 346-356	EPQVYTLPPSR*
16.8	1160.62 ± 0.22	1160.62	H 362-371	NQVSLTCLVK*
17.0	2622.21 ± 0.03	2622.21	H 99-122	TGWLGPFDYWGQGTLVTVSSAS TK**
17.1	1185.64 ± 0.18	1185.64	H 123-134	GPSVFPLAPSSK
18.4	2239.09 ± 0.60	2238.99	H 20-38	LSCAASGFTFSSYTMHWVR**
18.4	2800.24 ± 0.51	2800.26	H 418-440	WQQGNVFSCSVMHEALHNHYT QK*
18.5	2729.21 ± 0.02	2729.41	H 224-249	THTCPPCPAPELLGGPSVFLFPPK PK
18.5	2192.99 ± 0.29	2193.05	H 276-293	FNWYVDGVEVHNAKTKPR***
18.6	2573.09 ± 0.88	2579.05	H 372-393	GFYPSDIAVEWESNGQPENNYK* **
20.2	1872.91 ± 0.05	1872.91	H 394-410	TTPPVLDSDGSFFLYSK
21.0	2138.52 ± 0.22	2138.02	H 257-275	TPEVTCVVVDVSHEDPEVK*
23.1	3013.44 ± 0.05	3013.42	H 294-318	EEQYNSTYRVVSVLTVLHQDWL NGK***

conditions, by combining temperature (37 °C) and vigorous shaking (750 rpm). Indeed, the secondary and tertiary structure were preserved and the physical state (aggregation) did not change during the experiment. The presence of polysorbate 80 in the commercial formulation (Yervoy®) has likely protected the mAb from unfolding, aggregation, and precipitation. Indeed, polysorbates play a role in minimizing the effects of the mechanical stress, vortexing, freeze–thaw, and absorption to surfaces during protein therapeutic drug transportation and handling [38–41].

When stressed with 720 kJ/m^2 of artificial sunlight, a dose corresponding to the exposure criteria for ICH confirmatory photostability studies, Ipilimumab exhibited intensive aggregation and chemical modifications. This instability became dramatically evident after forced light doses (10460 kJ/m^2), leading to endangered monomeric species. As a matter of fact, Trp/Met oxidations and Gln/Asn deamidations were found. Therefore, the more hydrophilic oxidized and deamidated Ipilimumab interacted less strongly with the SEC stationary phase, thus decreasing the elution volume. The chemical modifications of the residues are quite critical since they can consistently affect the molecular physicochemical properties of protein in terms of hydrophobicity and charge. These in turn can modify both the analytical and the pharmacokinetics/pharmacodynamics properties of the drug [42] compromising its efficacy [17]. Protein oxidation increases side-chain hydrophilicity with an effect on the local flexibility, induces fragmentation, aggregation and cross-linking, protein unfolding and altered conformation, different interactions with biological partners and modified turnover [43]. Deamidation induces charge changes on the protein surface resulting in shifts of isoelectric point values and affecting the drug tissue distribution and kinetics [44]. Consequently, the chemical modifications can influence the stability of the protein native state, and therefore, they should be minimized or completely avoided using a suitable formulation composition. However, conformational changes were not evident and native secondary and tertiary structure was detectable by CD as already seen for other mAbs [45]. Notably, no turbidity, nor color change resulted under visual inspection of the irradiated samples in formulation.

Aggregation and chemical modifications were even higher when the drug formulation was diluted with 5% sterile glucose solution, usually employed for pediatric cases. In this context, Mittelmayer et al. [26] revealed that, during the sterilization step, glucose can generate degradation products (GDPs) able to react with active principles under light exposure. The dilution with a lab-made glucose solution

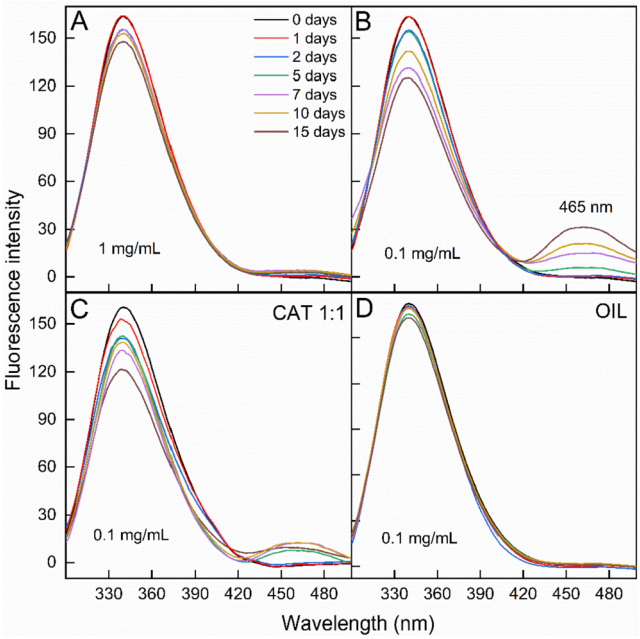

Fig. 8. Intrinsic fluorescence spectra of Ipilimumab samples obtained after dilution to 1 mg/ml (A), and 0.1 mg/ml (B) in 0.9 % saline solution for the specified times of incubation. Spectra recorded in the presence of catalase (C) or covering the samples with mineral oil (D) were reported. Excitation wavelength was at 280 nm.

highlighted the role of glucose side products known to be formed under heat sterilization and responsible for further protein damage under light. As a matter of fact, the mAb was much more stable in this last dilution and in saline solution.

Under the light stressor, polysorbate 80 might play a role in inducing protein instability. Its susceptibility to auto-oxidation and hydrolysis can facilitate the degradation of proteins [46]. Exposed to light, this surfactant undergoes autoxidation of the polyoxyethylene chain, leading to the formation of hydroperoxide derivatives, able to cause oxidative damage of the most sensitive amino acids in the formulated protein molecules [22]. It is noteworthy that Ipilimumab stressed by light in the formulation was not cytotoxic when tested on two cell lines despite the observed modification of the mAb.

As an additional stressor test, the effect of dilution on the formulation was monitored by using a saline solution (1 mg/mL Ipilimumab), which is the most used during hospital infusion. After two days from dilution, protein aggregation started to appear but did not evolve further. However, the protein exhibited chemical modifications including oxidation and deamidation. The loss of the critical concentration of polysorbate 80 could explain the effects induced by dilution on the formulation. Indeed, it was previously demonstrated that the presence of a threshold level of polysorbate (20 or 80) is important to guarantee protein stability [47]. Moreover, during the dilution, a larger relative proportion of the protein may be located at the air–water interface, partly due to a lower protein concentration and partly due to a lower polysorbate concentration. This could induce a partial protein unfolding thus making the macromolecule more susceptible to oxidation [48]. Following the polysorbate auto-oxidation, triggered by the reduction of its critical concentration, the development of degradation products such as peroxides, ketones,

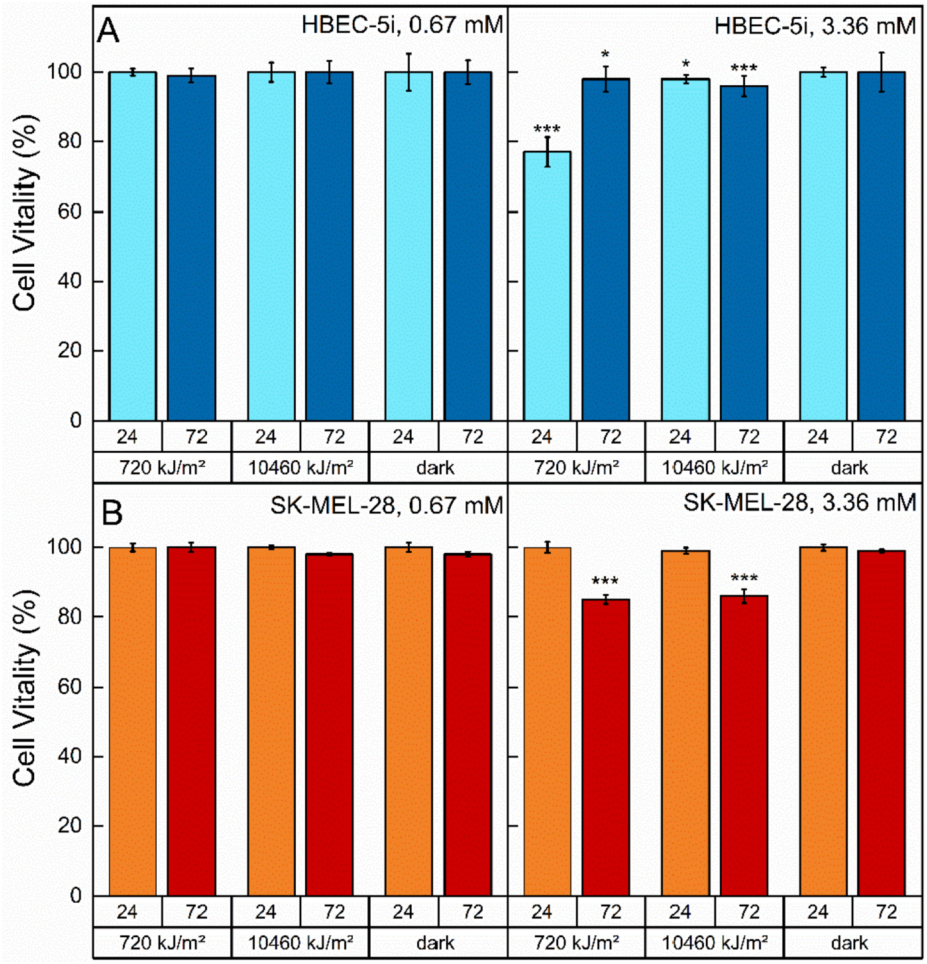

Fig. 9. Cytotoxicity of Ipilimumab samples after exposure under 720 and 10460 kJ/m^2 of artificial sunlight in comparison to the dark control by Preston Blue assay. Viability of HBEC-5i (A) and SK-MEL-28 (B) cells exposed for 24 and 72 h to 0.67 mM (left) and 3.36 mM (right) of Ipilimumab. Error bars indicated the standard errors of three independent experiments carried out in triplicate. Statistically relevant variations are indicated by stars, *** $p < 0.001$, ** $p < 0.01$, * $p < 0.05$. (For interpretation of the references to color in this figure legend, the reader is referred to the web version of this article.)

aldehydes, or fatty acid esters occurs, and it could promote the oxidation of amino acid residues [46]. This was here demonstrated by the significant decrease and even absence of fluorescence signal due to oxidative processes after catalase or oil addition, respectively.

Taken together, our results suggest that special warning must be paved on protein aggregation phenomena, which could compromise not only the efficacy of the drug itself but also its correct administration to the patient (i.e., obstruction of needles and lines). Yervoy appeared to be a photolabile formulation before and after dilution and should be always stored protected from light. Special protection should be considered even during the prolonged infusion step to the patient.

5. Conclusions

This work aimed to provide a deeper understanding of the post-production and handling phases of a biologic product, by highlighting both the intrinsic fragility of a mAb and the difficulty to create a formulation to overcome delivery, storage, and administration issues. In particular, the stability of Ipilimumab in several types of stress conditions was tested, performing analyses with a broad variety of analytical techniques. Additionally, the influence of glucose solutions on the stability/photostability of the protein drug has been here demonstrated for the first time, suggesting evaluating with special care the use of glucose solutions for the dilution/reconstitution of the mAbs before their administration to the patients. Moreover, extended in-use stability of diluted biotechnological formulations could help pharmacists to optimize hospital expenses of these costly drugs. The hope is that this work may be useful to evaluate the concerns relative to everyday hospital handling and overall raise awareness on the proper use and storage of biotechnological therapeutic drugs.

Declaration of Competing Interest

The authors declare that they have no known competing financial interests or personal relationships that could have appeared to influence the work reported in this paper.

Acknowledgement

This work was supported by IMI Project: Real World Handling of Protein Drugs-Exploration, Evaluation and Education - RealHOPE No. 101007939. We thank Dr. Marino Bellini for the technical assistance in mass spectrometry.

Appendix A. Supplementary material

Supplementary data to this article can be found online at https://doi.org/10.1016/j.ejpb.2022.05.005.

References

[1] L.M. Weiner, Cancer immunology for the clinician, Clin Adv Hematol Oncol. 13 (2015) 299–306.
[2] J. Zugazagoitia, C. Guedes, S. Ponce, I. Ferrer, S. Molina-Pinelo, L. Paz-Ares, Current Challenges in Cancer Treatment, Clin Ther. 38 (2016) 1551–1566, https://doi.org/10.1016/j.clinthera.2016.03.026.
[3] P. Darvin, S.M. Toor, V. Sasidharan Nair, E. Elkord, Immune checkpoint inhibitors: recent progress and potential biomarkers, Exp Mol Med. 50 (2018) 1–11, https://doi.org/10.1038/s12276-018-0191-1.
[4] European Pharmacopoeia (Ph. Eur.) 8th Edition: General Monographs n.2031 Anticorpora monoclonalia ad usum humanum.
[5] L.M. Weiner, R. Surana, S. Wang, Monoclonal antibodies: versatile platforms for cancer immunotherapy, Nat Rev Immunol. 10 (2010) 317–327, https://doi.org/10.1038/nri2744.
[6] G.J. Weiner, Monoclonal antibody mechanisms of action in cancer, Immunol Res 39 (2007) 271–278, https://doi.org/10.1007/s12026-007-0073-4.
[7] H. Lee, S. Lee, Y.-S. Heo, Molecular Interactions of Antibody Drugs Targeting PD-1, PD-L1, and CTLA-4 in Immuno-Oncology, Molecules 24 (6) (2019) 1190.
[8] A. Gadducci, M.E. Guerrieri, Immune Checkpoint Inhibitors in Gynecological Cancers: Update of Literature and Perspectives of Clinical Research, Anticancer Res. 37 (2017) 5955–5965, https://doi.org/10.21873/anticanres.12042.
[9] J.D. Wolchok, B. Neyns, G. Linette, S. Negrier, J. Lutzky, L. Thomas, W. Waterfield, D. Schadendorf, M. Smylie, T. Guthrie, J.-J. Grob, J. Chesney, K. Chin, K. Chen, A. Hoos, S.J. O'Day, C. Lebbé, Ipilimumab monotherapy in patients with pretreated advanced melanoma: a randomised, double-blind, multicentre, phase 2, dose-ranging study, Lancet Oncol. 11 (2) (2010) 155–164.
[10] F.S. Hodi, S.J. O'Day, D.F. McDermott, R.W. Weber, J.A. Sosman, J.B. Haanen, R. Gonzalez, C. Robert, D. Schadendorf, J.C. Hassel, W. Akerley, A.J.M. van den Eertwegh, J. Lutzky, P. Lorigan, J.M. Vaubel, G.P. Linette, D. Hogg, C. H. Ottensmeier, C. Lebbé, C. Peschel, I. Quirt, J.I. Clark, J.D. Wolchok, J.S. Weber, J. Tian, M.J. Yellin, G.M. Nichol, A. Hoos, W.J. Urba, Improved survival with ipilimumab in patients with metastatic melanoma, N Engl J Med. 363 (8) (2010) 711–723.
[11] J.F. Grosso, M.N. Jure-Kunkel, CTLA-4 blockade in tumor models: an overview of preclinical and translational research, Cancer Immun. 13 (2013) 5.
[12] U.A. Ramagopal, W. Liu, S.C. Garrett-Thomson, J.B. Bonanno, Q. Yan, M. Srinivasan, S.C. Wong, A. Bell, S. Mankikar, V.S. Rangan, S. Deshpande, A. J. Korman, S.C. Almo, Structural basis for cancer immunotherapy by the first-in-class checkpoint inhibitor ipilimumab, Proc Natl Acad Sci U S A. 114 (21) (2017), https://doi.org/10.1073/pnas.1617941114.
[13] F. Cymer, H. Beck, A. Rohde, D. Reusch, Therapeutic monoclonal antibody N-glycosylation - Structure, function and therapeutic potential, Biologicals. 52 (2018) 1–11, https://doi.org/10.1016/j.biologicals.2017.11.001.
[14] Yervoy, INN-ipilimumab Annex I summary of product characteristics. https://www.ema.europa.eu/en/documents/product-information/yervoy-epar-product-information_en.pdf.
[15] M.C. Manning, D.K. Chou, B.M. Murphy, R.W. Payne, D.S. Katayama, Stability of protein pharmaceuticals: an update, Pharm Res. 27 (2010) 544–575, https://doi.org/10.1007/s11095-009-0045-6.
[16] J. Li, M.E. Krause, X. Chen, Y. Cheng, W. Dai, J.J. Hill, M. Huang, S. Jordan, D. LaCasse, L. Narhi, E. Shalaev, I.C. Shieh, J.C. Thomas, R. Tu, S. Zheng, L. Zhu, Interfacial Stress in the Development of Biologics: Fundamental Understanding, Current Practice, and Future Perspective, AAPS J. 21 (3) (2019), https://doi.org/10.1208/s12248-019-0312-3.
[17] S. Gupta, W. Jiskoot, C. Schöneich, A.S. Rathore, Oxidation and Deamidation of Monoclonal Antibody Products: Potential Impact on Stability, Biological Activity, and Efficacy, J Pharm Sci 111 (4) (2022) 903–918.
[18] M.J. Davies, The oxidative environment and protein damage, Biochim Biophys Acta. 1703 (2005) 93–109, https://doi.org/10.1016/j.bbapap.2004.08.007.
[19] M.J. Davies, Singlet oxygen-mediated damage to proteins and its consequences, Biochem. Biophys. Res. Commun. 305 (2003) 761–770, https://doi.org/10.1016/S0006-291X(03)00817-9.
[20] A. Sreedhara, J. Yin, M. Joyce, K. Lau, A.T. Wecksler, G. Deperalta, L. Yi, Y. J. Wang, B. Kabakoff, R.S.K. Kishore, Effect of ambient light on IgG1 monoclonal antibodies during drug product processing and development, Eur J Pharm Biopharm. 100 (2016) 38–46, https://doi.org/10.1016/j.ejpb.2015.12.003.
[21] B.A. Kerwin, R.L. Remmele, Protect from light: photodegradation and protein biologics, J Pharm Sci. 96 (6) (2007) 1468–1479.
[22] S.R. Singh, J. Zhang, C. O'Dell, M.-C. Hsieh, J. Goldstein, J. Liu, A. Srivastava, Effect of polysorbate 80 quality on photostability of a monoclonal antibody, AAPS PharmSciTech. 13 (2012) 422–430, https://doi.org/10.1208/s12249-012-9759-6.
[23] C. Bardin, A. Astier, A. Vulto, G. Sewell, J. Vigneron, R. Trittler, M. Daouphars, M. Paul, M. Trojniak, F. Pinguet, Guidelines for the practical stability studies of anticancer drugs: a European consensus conference, Ann Pharm Fr. 69 (4) (2011) 221–231.
[24] M. Paul, V. Vieillard, E. Jaccoulet, A. Astier, Long-term stability of diluted solutions of the monoclonal antibody rituximab, Int J Pharm. 436 (2012) 282–290, https://doi.org/10.1016/j.ijpharm.2012.06.063.
[25] European Pharmacopoeia (Ph. Eur.) 9th Edition: Monograph 5.1.1 Methods of Preparation of Sterile Products; 2017.
[26] S. Mittelmaier, M. Fünfrocken, D. Fenn, T. Fichert, M. Pischetsrieder, Identification and quantification of the glucose degradation product glucosone in peritoneal dialysis fluids by HPLC/DAD/MSMS, J Chromatogr B Analyt Technol Biomed Life Sci. 878 (2010) 877–882, https://doi.org/10.1016/j.jchromb.2010.02.004.
[27] A.M. Taher, D.M. Cates, A spectrophotometric investigation of the yellow color that accompanies the formation of furan derivatives in degraded-sugar solutions, Carbohydr. Res. 34 (1974) 249–261, https://doi.org/10.1016/S0008-6215(00)82900-6.
[28] R. Ulbricht, A review of 5-hydroxymethylfurfural (HMF) in parenteral solutions, Fundam. Appl. Toxicol. 4 (1984) 843–853, https://doi.org/10.1016/0272-0590(84)90106-4.
[29] E. Li, N.i. Lin, R. Hao, X. Fan, L. Lin, G. Hu, S. Lin, J. He, Q. Zhu, H. Jin, 5-HMF induces anaphylactoid reactions in vivo and in vitro, Toxicol Rep. 7 (2020) 1402–1411.
[30] J. Brustugun, H.H. Tønnesen, R. Edge, S. Navaratnam, Formation and reactivity of free radicals in 5-hydroxymethyl-2-furaldehyde–the effect on isoprenaline photostability, J Photochem Photobiol B. 79 (2005) 109–119, https://doi.org/10.1016/j.jphotobiol.2004.12.005.
[31] U.K. Laemmli, Cleavage of structural proteins during the assembly of the head of bacteriophage T4, Nature 227 (1970) 680–685, https://doi.org/10.1038/227680a0.
[32] R. Ragone, G. Colonna, C. Balestrieri, L. Servillo, G. Irace, Determination of tyrosine exposure in proteins by second-derivative spectroscopy, Biochemistry 23 (1984) 1871–1875, https://doi.org/10.1021/bi00303a044.

[33] S.C. Gill, P.H. von Hippel, Calculation of protein extinction coefficients from amino acid sequence data, Anal Biochem. 182 (2) (1989 Nov 1) 319–326, https://doi.org/10.1016/0003-2697(89)90602-7. Erratum. In: Anal Biochem 1990 Sep; 189(2): 283.
[34] A. Goyon, V. D'Atri, O. Colas, S. Fekete, A. Beck, D. Guillarme, Characterization of 30 therapeutic antibodies and related products by size exclusion chromatography: Feasibility assessment for future mass spectrometry hyphenation, J Chromatogr B Analyt Technol Biomed Life Sci. 1065–1066 (2017) 35–43, https://doi.org/10.1016/j.jchromb.2017.09.027.
[35] C.A. Royer, Probing Protein Folding and Conformational Transitions with Fluorescence, Chem. Rev. 106 (5) (2006) 1769–1784.
[36] S. Leitzen, M. Vogel, M. Steffens, T. Zapf, C.E. Müller, M. Brandl, Quantification of Degradation Products Formed during Heat Sterilization of Glucose Solutions by LC-MS/MS: Impact of Autoclaving Temperature and Duration on Degradation, Pharmaceuticals 14 (2021) 1121, https://doi.org/10.3390/ph14111121.
[37] P. Bardo-Brouard, V. Vieillard, T. Shekarian, A. Marabelle, A. Astier, M. Paul, Stability of ipilimumab in its original vial after opening allows its use for at least 4 weeks and facilitates pooling of residues, Eur J Cancer. 58 (2016) 8–16, https://doi.org/10.1016/j.ejca.2016.01.008.
[38] T.A. Khan, H.-C. Mahler, R.S.K. Kishore, Key interactions of surfactants in therapeutic protein formulations: A review, Eur J Pharm Biopharm. 97 (2015) 60–67, https://doi.org/10.1016/j.ejpb.2015.09.016.
[39] D.K. Chou, R. Krishnamurthy, T.W. Randolph, J.F. Carpenter, M.C. Manning, Effects of Tween 20 and Tween 80 on the stability of Albutropin during agitation, J Pharm Sci. 94 (2005) 1368–1381, https://doi.org/10.1002/jps.20365.
[40] W. Liu, D.Q. Wang, S.L. Nail, Freeze-drying of proteins from a sucrose-glycine excipient system: effect of formulation composition on the initial recovery of protein activity, AAPS PharmSciTech. 6 (2005) E150–E157, https://doi.org/10.1208/pt060223.
[41] H.-C. Mahler, F. Huber, R.S.K. Kishore, J. Reindl, P. Rückert, R. Müller, Adsorption behavior of a surfactant and a monoclonal antibody to sterilizing-grade filters, J Pharm Sci. 99 (2010) 2620–2627, https://doi.org/10.1002/jps.22045.
[42] M.L. Chiu, D.R. Goulet, A. Teplyakov, G.L. Gilliland, Antibody Structure and Function: The Basis for Engineering Therapeutics, Antibodies (Basel) 8 (4) (2019) 55.
[43] M.J. Davies, Protein oxidation and peroxidation, Biochem J. 473 (2016) 805–825, https://doi.org/10.1042/BJ20151227.
[44] D. Chelius, D.S. Rehder, P.V. Bondarenko, Identification and characterization of deamidation sites in the conserved regions of human immunoglobulin gamma antibodies, Anal Chem. 77 (2005) 6004–6011, https://doi.org/10.1021/ac050672d.
[45] M. Agarkhed, C. O'Dell, M.-C. Hsieh, J. Zhang, J. Goldstein, A. Srivastava, Effect of polysorbate 80 concentration on thermal and photostability of a monoclonal antibody, AAPS PharmSciTech. 14 (2013) 1–9, https://doi.org/10.1208/s12249-012-9878-0.
[46] N.R. Larson, Y. Wei, I. Prajapati, A. Chakraborty, B. Peters, C. Kalonia, S. Hudak, S. Choudhary, R. Esfandiary, P. Dhar, C. Schöneich, C.R. Middaugh, Comparison of Polysorbate 80 Hydrolysis and Oxidation on the Aggregation of a Monoclonal Antibody, J Pharm Sci. 109 (1) (2020) 633–639.
[47] R.S.K. Kishore, S. Kiese, S. Fischer, A. Pappenberger, U. Grauschopf, H.-C. Mahler, The degradation of polysorbates 20 and 80 and its potential impact on the stability of biotherapeutics, Pharm Res. 28 (2011) 1194–1210, https://doi.org/10.1007/s11095-011-0385-x.
[48] E. D'Imprima, D. Floris, M. Joppe, R. Sánchez, M. Grininger, W. Kühlbrandt, Protein denaturation at the air-water interface and how to prevent it, Elife (2019), https://doi.org/10.7554/eLife.42747.001.